

Application of computer models for advancement of X-ray breast imaging techniques

Grand Hotel Santa Lucia Napoli

Phase contrast mammography with synchrotron radiation

Alberto Bravin

European Synchrotron Radiation Facility (Grenoble, France)



To MAXIMA organizers for their kind invitation

To all collaborators

A special thanks to:

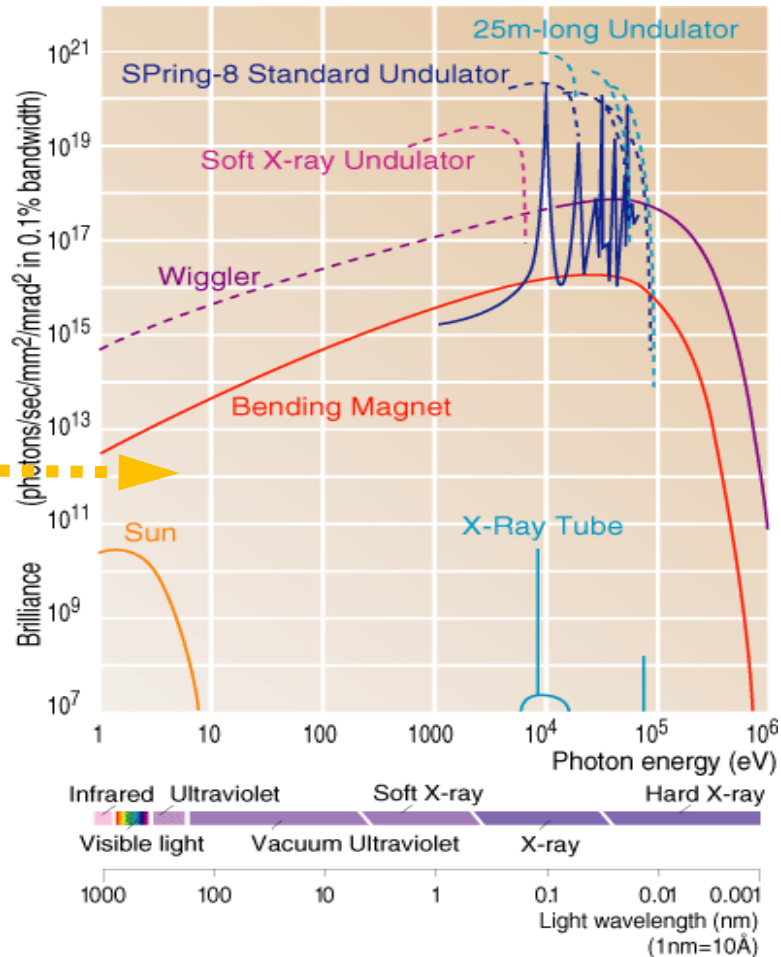
- Prof. Paola COAN, LMU, Munich
- Dr. Alberto MITTONE, ESRF
- Prof. T. Peters, London, Canada

“A very large microscope to see deep inside matter”

- **A source of X-rays produced by relativistic electrons of special characteristics:**
- **Extremely intense: the most intense on earth**
- **Highly collimated**
- **Brilliant**
- **Tunable in energy**



SYNCHROTRON RADIATION FOR MEDICAL APPLICATIONS



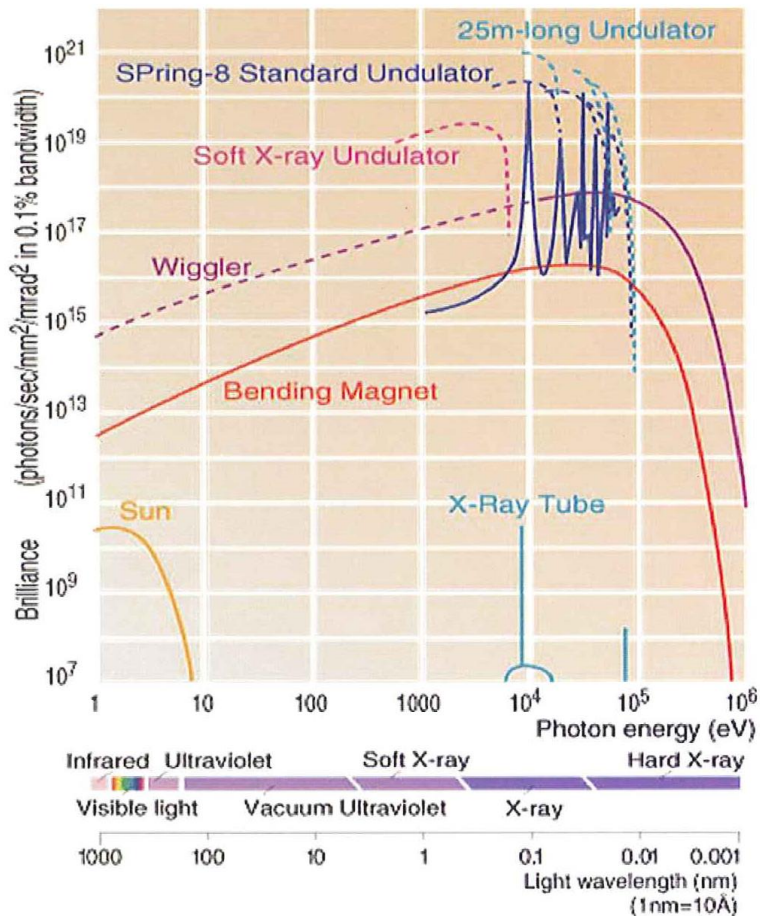
Why is SR interesting for imaging and therapy?

- $\sim 10^6/10^8$ more intense than medical X-ray generators or LINACS
- tunable monochromatic energy
- parallel beam
- (sub)micrometric spatial resolution

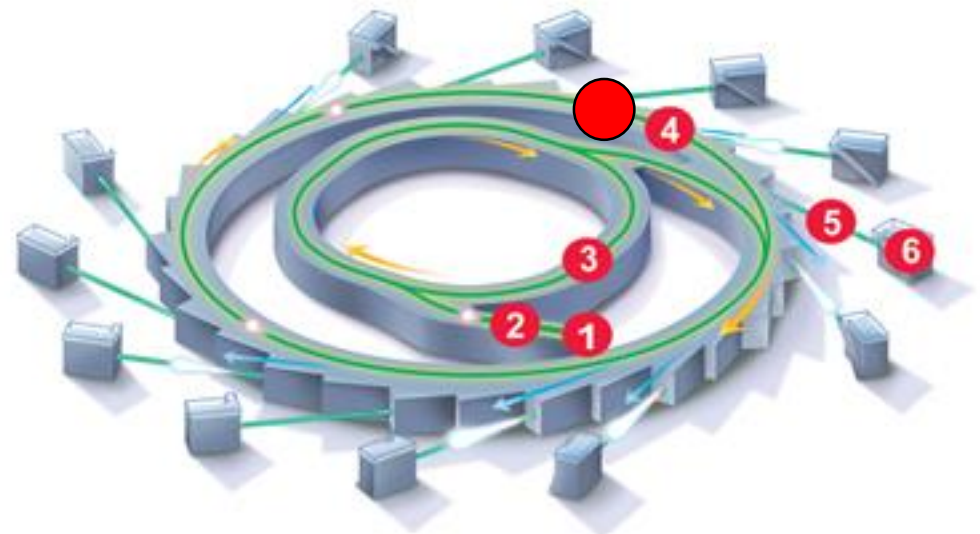
HOW IS A SYNCHROTRON MADE?

SR is a very intense source of radiation from Infra Red to hard X-rays

SR is produced by electrons with relativistic energies circulating in a ring



Synchrotron machine scheme

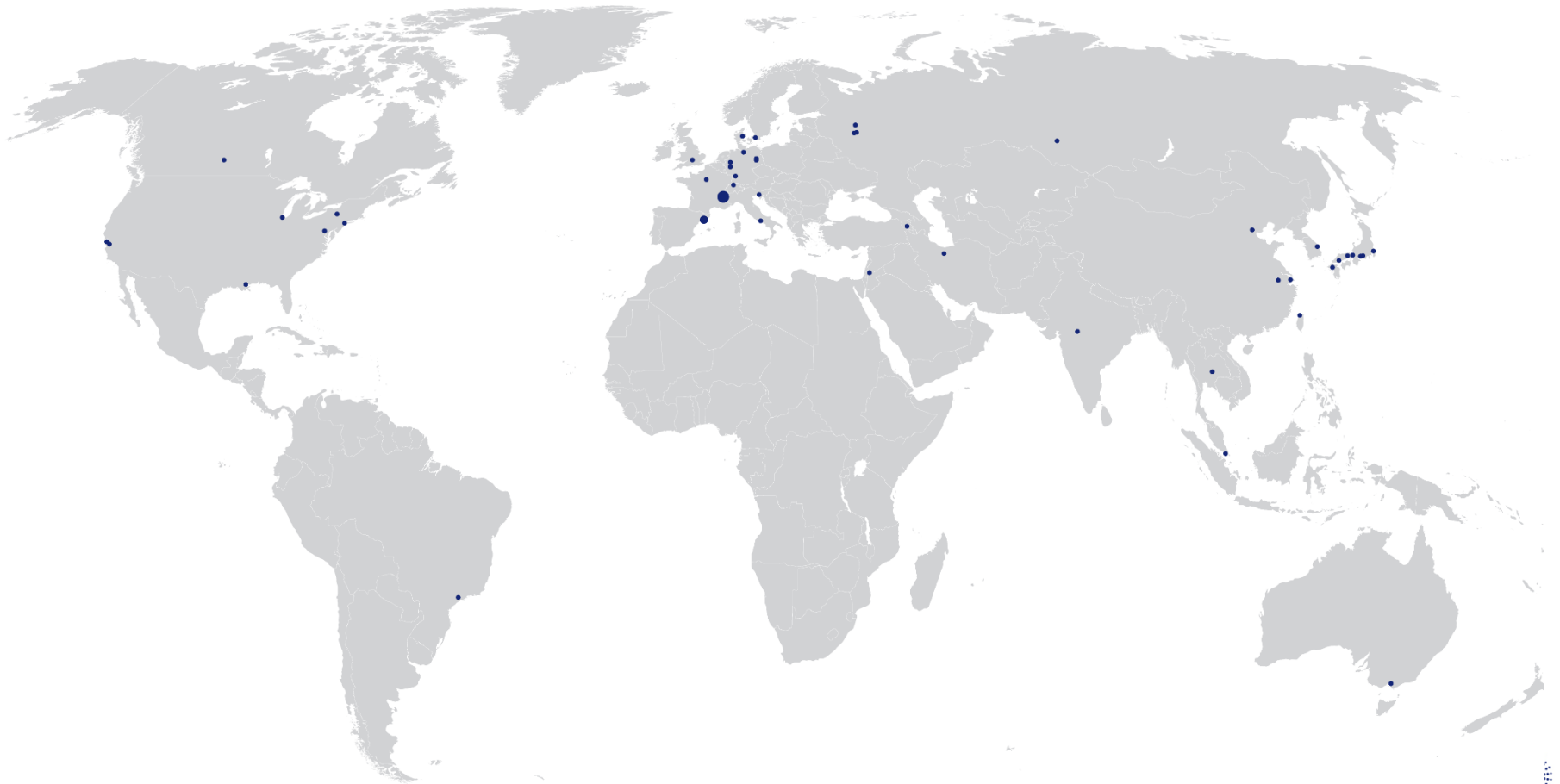


1 injector 2 transfer line 3 booster
4 storage ring 5 beamline 6 exp. station

SYNCHROTRONS IN THE WORLD

3 larger facilities

5 with dedicated medical beamlines



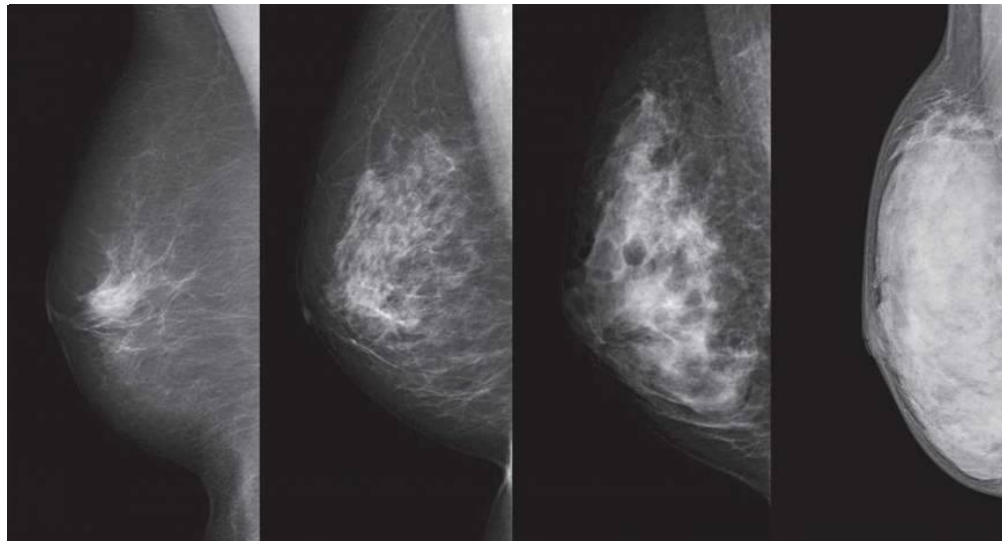
LIMITS OF CONVENTIONAL X-RAY RADIOGRAPHY IN BREAST IMAGING

Breast cancer: First mortality cause for women in western countries



Diagnosis is simple in a fatty breast (radiotransparent)

90%/10% — Fat - Glandular tissues —> 10%/90%



Tumors in dense breasts are masked by tissues

Challenges in mammography

“ ~10% of palpable malignant tumours are not visible in mammography (dense breast, infiltrating tumors etc)”

- **High radiosensitive organ**
--> Possible radio-induced tumors -- > Risk benefit evaluation
- **Small difference in contrast between tumor and normal tissues**
-- > need more images, higher doses
- **Need of resolutions better/= 40 microns (microcalcifications)**
-- > doses increase with the $1/\text{pixel}^2$
- **Need of better identification of the lesion (2.5D – 3D imaging)**
--> higher doses

- **Improve contrast formation**: from absorption to phase contrast imaging
-- > use improved source or setup (**Olivo, Longo, Bravin, Paterno...**)
- **Move from 2D to 2.5 and 3D**: vision in depth
-- > tomosynthesis or CT (**K. Bliznakova**)
- **Improve detectors** -- > higher efficiency of used dose
-- > single photon counting (**Kalender, Boone, Esposito..**)
- **Improve image reconstruction** technique to use fewer X-rays and reduce dose
-- > use improved reconstruction algorithms (**This talk**)

A software platform for phase contrast x-ray breast imaging research

K. Bliznakova^{a,*}, P. Russo^b, G. Mettivier^b, H. Requardt^c, P. Popov^d, A. Bravin^c, I. Buliev^a

^a Department of Electronics, Technical University of Varna, 1 Studentska Str, Varna 9010, Bulgaria

^b Dipartimento di Fisica, Università di Napoli Federico II, and INFN Sezione di Napoli, Via Cintia, I-80126 Naples, Italy

^c European Synchrotron Radiation Facility (ESRF), Grenoble F-38043, France

^d Department of Physics, Technical University of Varna, 1 Studentska Str, Varna 9010, Bulgaria

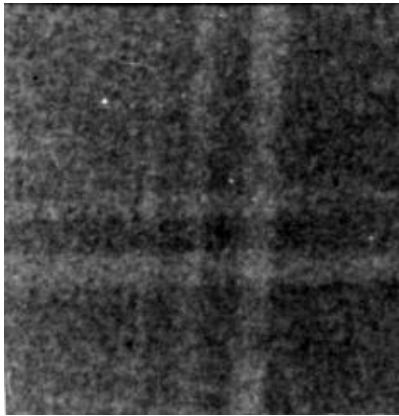
In-line phase-contrast breast tomosynthesis: a phantom feasibility study at a synchrotron radiation facility

K Bliznakova¹, P Russo², Z Kamarianakis⁴, G Mettivier²,
H Requardt³, A Bravin³ and I Buliev¹

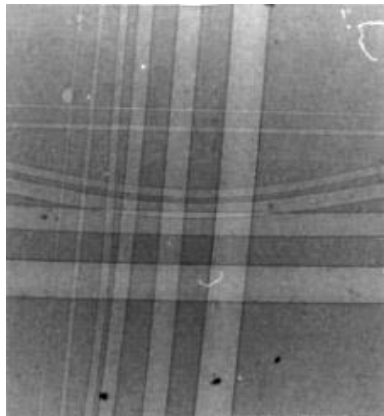
Phys. Med. Biol. 61 (2016) 6243–6263

PHC IN THE 90IES: FROM NYLON WIRES TO FIRST MAMMOGRAPHIES

Conventional
radiography



Phase
contrast



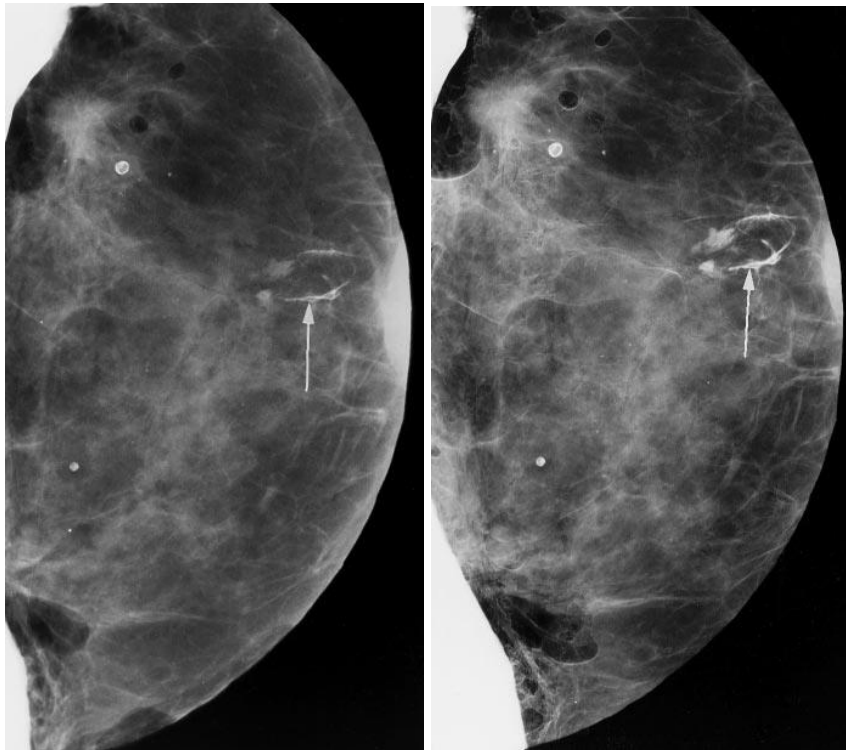
Elettra synchrotron
1997-1998

*F. Arfelli, A. Bravin et al,
Physics in Medicine and Biology 43, 1998*



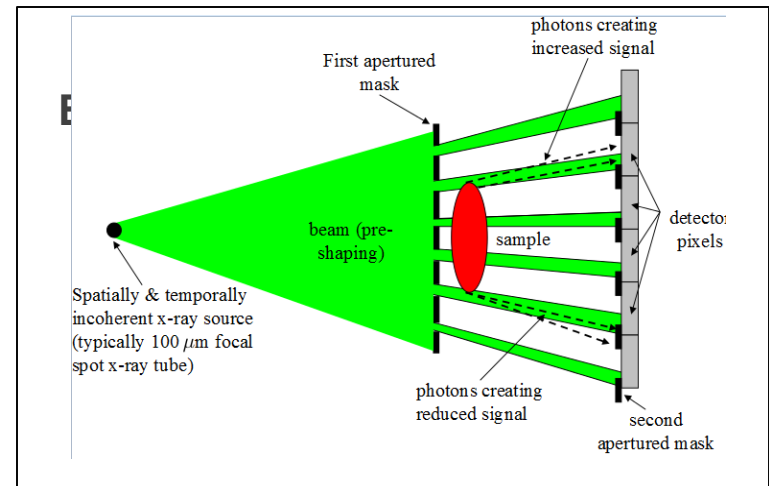
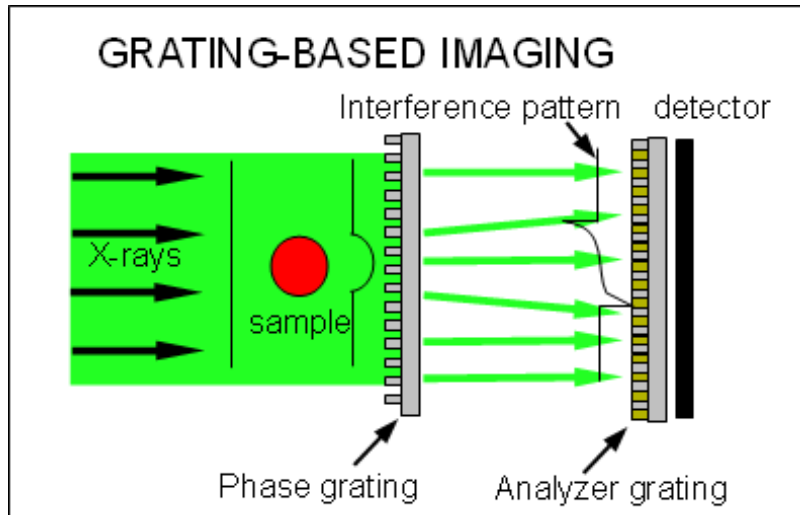
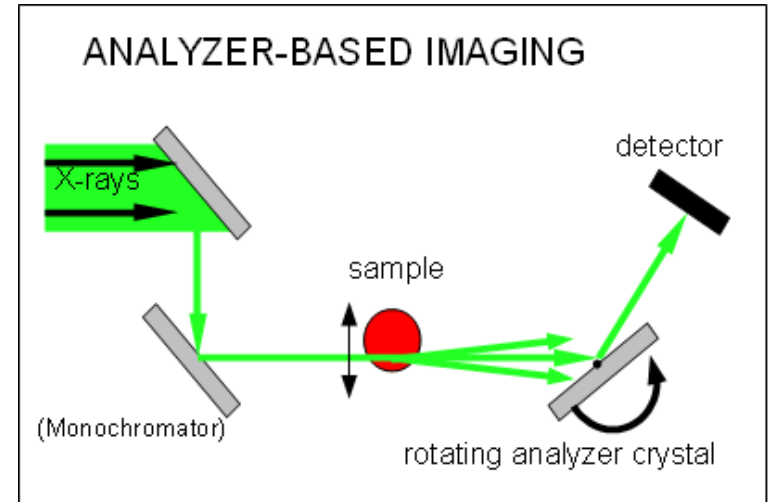
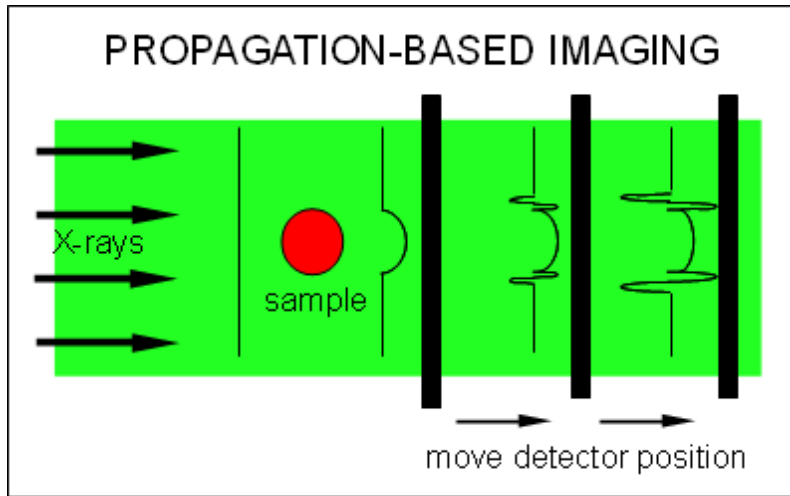
“Yes, but it can work only in simple objects”

First demonstration of phase contrast
imaging in a full human organ



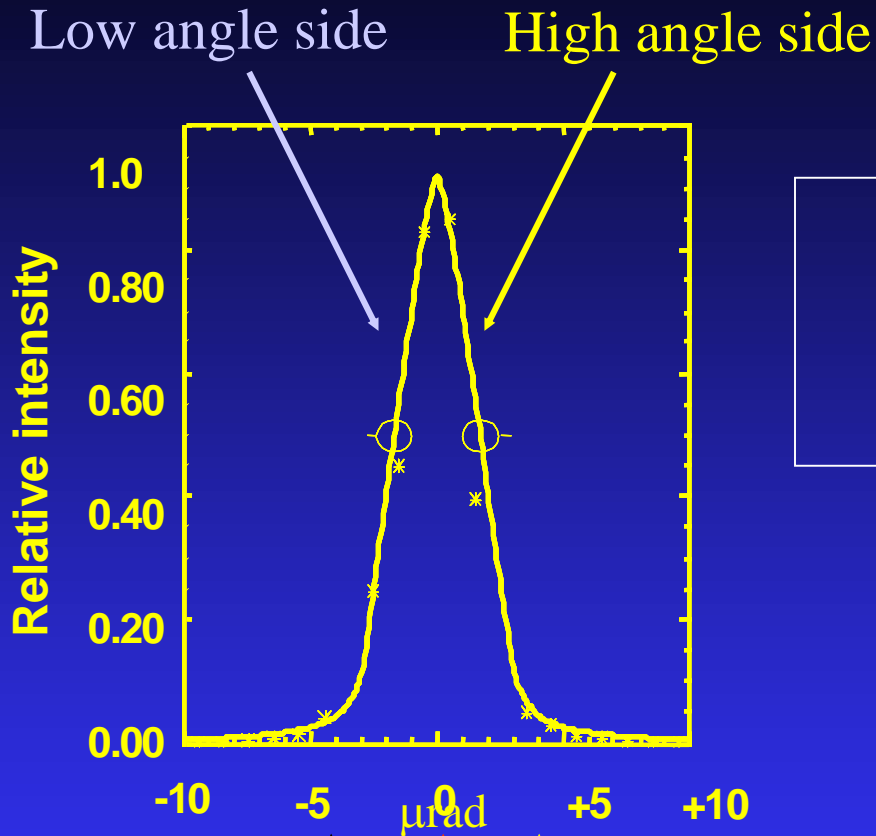
*F. Arfelli, A. Bravin et al,
Radiology 215, 2000*

TECHNIQUES AVAILABLE FOR PHASE CONTRAST IMAGING



Optimal radiation is monochromatic collimated, and coherent X-rays, presently available only at **synchrotron radiation sources**

Analyzer-Based Imaging (ABI)



Analyzer:
acts as a perfect and
extremely narrow slit

Rocking curve width Si (333)

~ 3.0 μrad at 25 keV

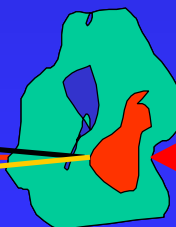
~ 1.3 μrad at 50 keV

~ 0.9 μrad at 60 keV

Bragg's law:
 $2d\sin\theta = n\lambda$

Analyzer crystal

δ^+

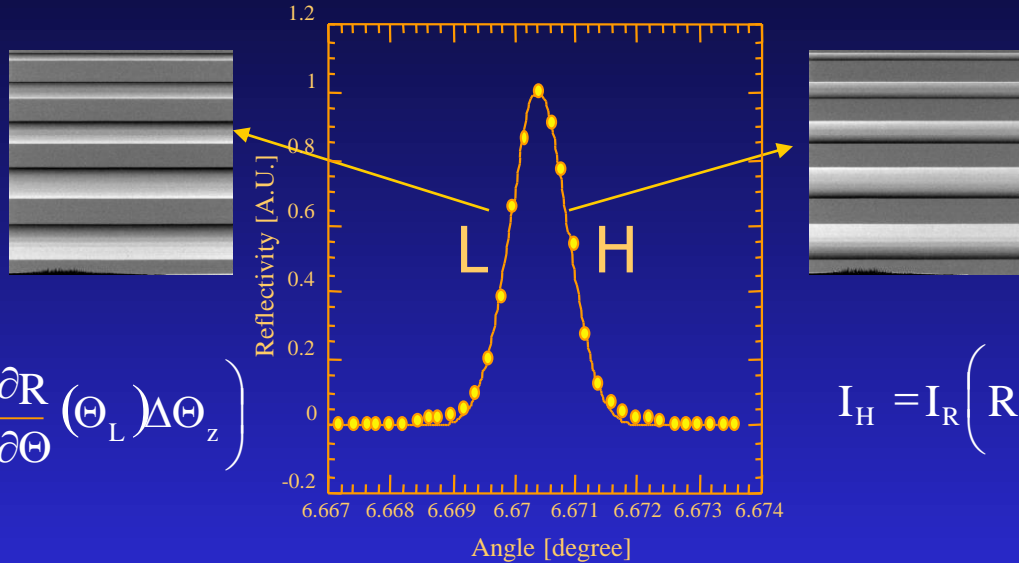


Sample

Incoming beam

δ^-

Diffraction Enhanced Imaging: an algorithm for ABI



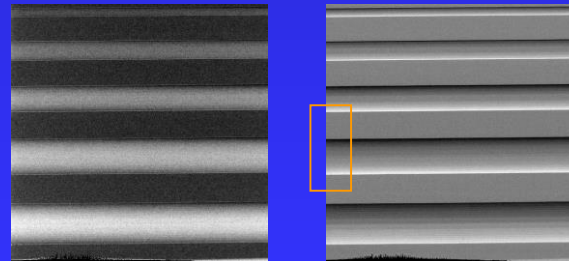
$$I_L = I_R \left(R(\Theta_L) + \frac{\partial R}{\partial \Theta}(\Theta_L) \Delta \Theta_Z \right)$$

$$I_H = I_R \left(R(\Theta_H) + \frac{\partial R}{\partial \Theta}(\Theta_H) \Delta \Theta_Z \right)$$

I_R = apparent absorption image

$\Delta \Theta_Z$ = refraction image in the plane of the object

$$I_R = \frac{I_L \cdot \left. \frac{dR}{d\Theta} \right|_{\Theta_H} - I_H \cdot \left. \frac{dR}{d\Theta} \right|_{\Theta_L}}{R(\Theta_L) \cdot \left. \frac{dR}{d\Theta} \right|_{\Theta_H} - R(\Theta_H) \cdot \left. \frac{dR}{d\Theta} \right|_{\Theta_L}}$$



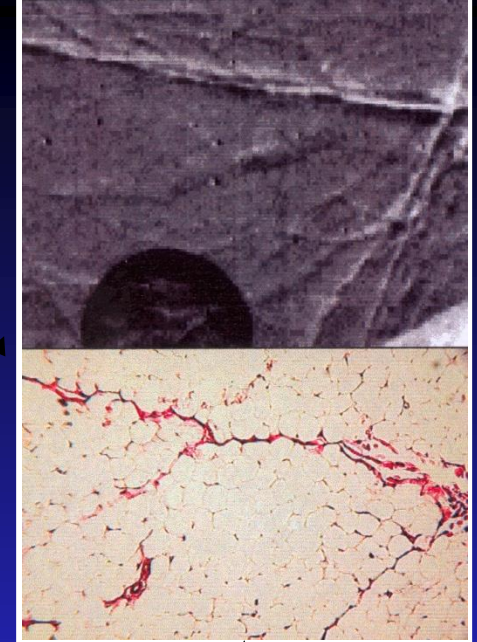
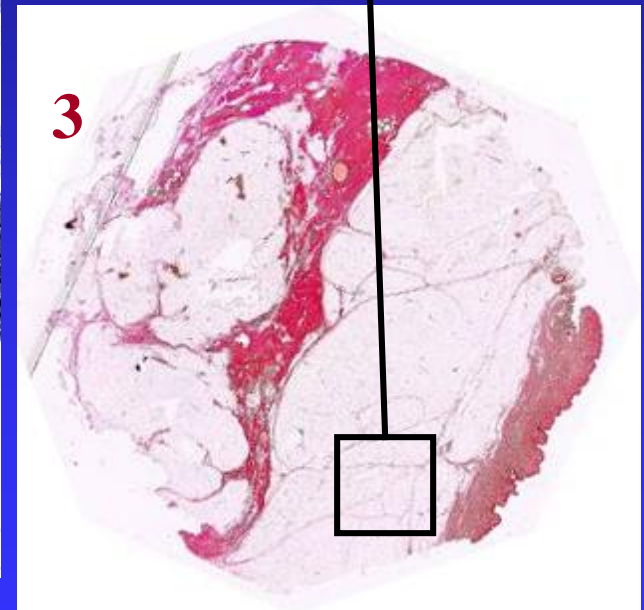
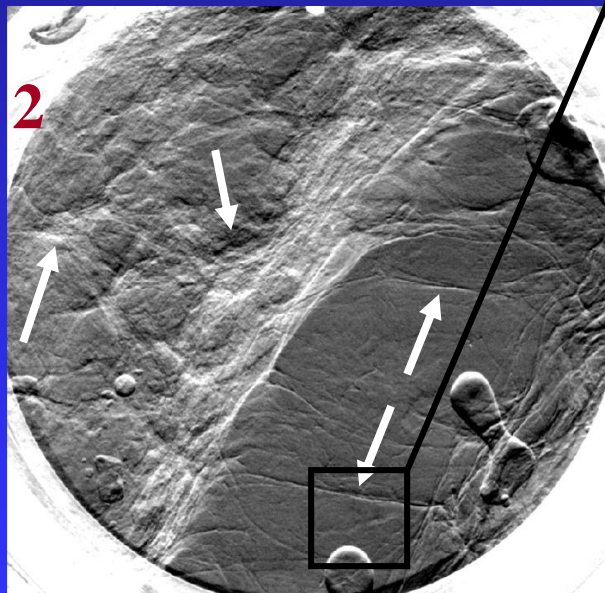
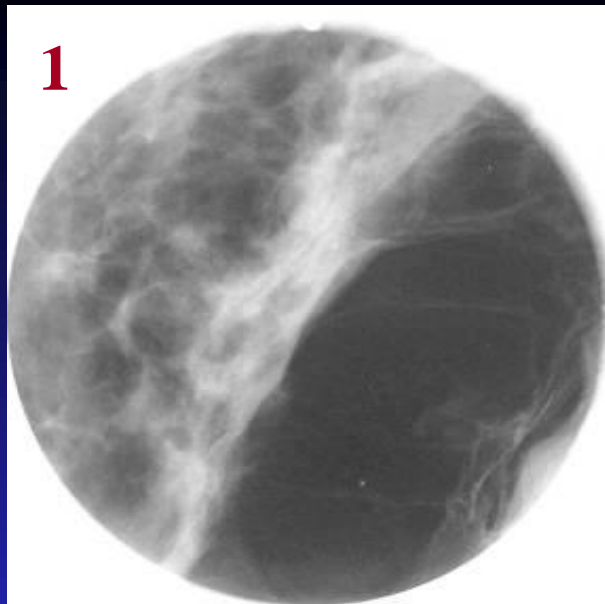
$$\Delta \Theta_Z = \frac{I_H \cdot R(\Theta_L) - I_L \cdot R(\Theta_H)}{I_L \cdot \left. \frac{dR}{d\Theta} \right|_{\Theta_H} - I_H \cdot \left. \frac{dR}{d\Theta} \right|_{\Theta_L}}$$

Carcinoma Medullare

- 1 Siemens
Mammomat
3000 -23 kVp
5.6 mAs
MGD=0.4 mGy

- 2 ABI 25 keV
minus 0.7 μ rad
Si(333)
MGD= 0.6 mGy

- 3 Histology

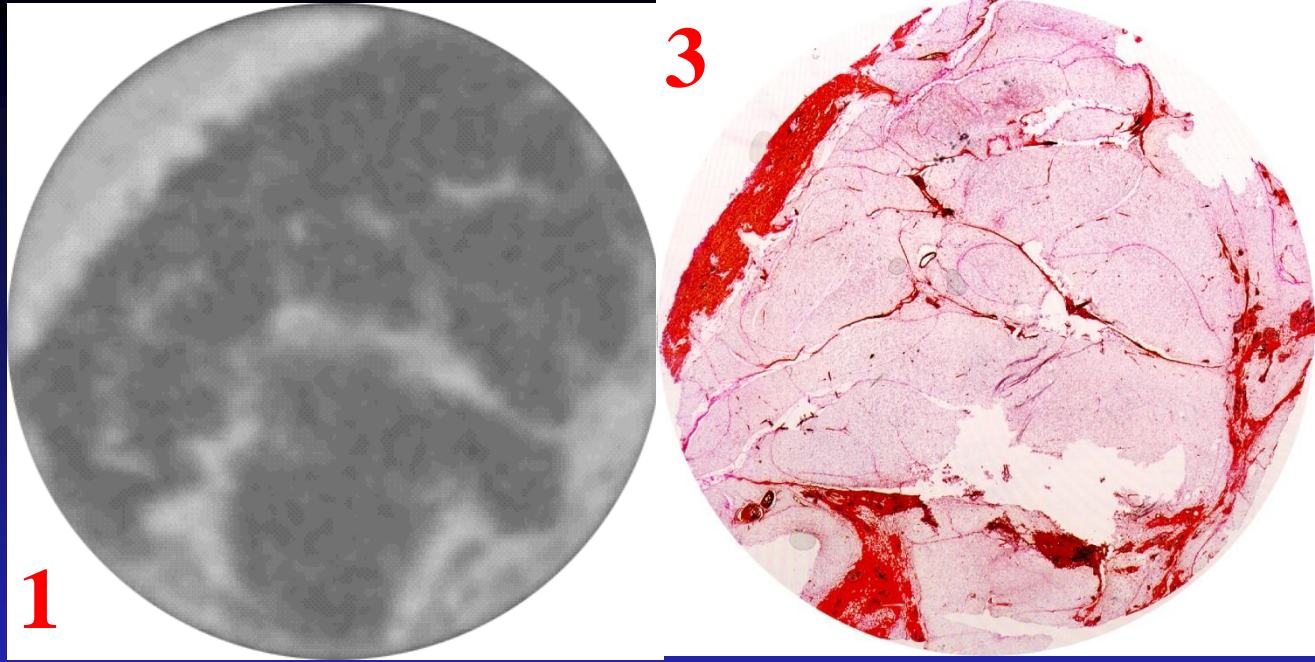


Keyriläinen et al. European Journal of Radiology 53, 226-237 (2005)

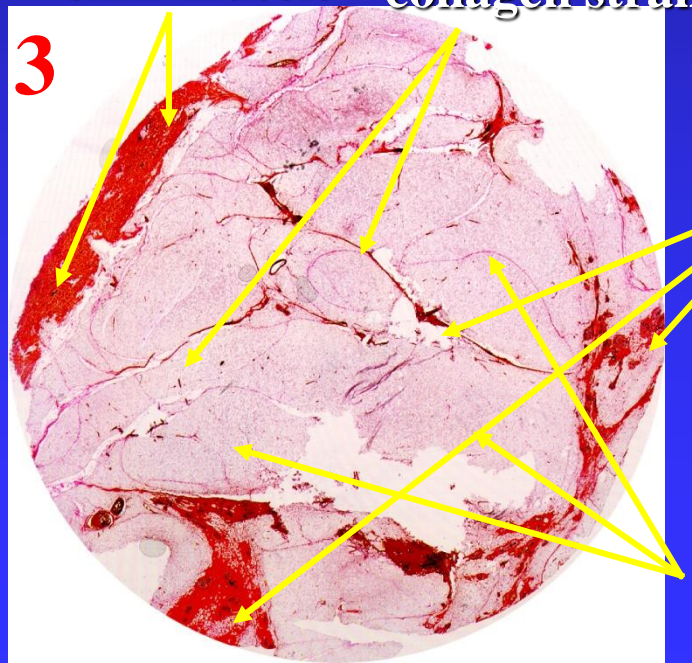
ABI-CT

Breast cancer

- 1 Hospital scanner
- 2 SR technique
- 3 Histology (reality)



skin-muscle collagen strands

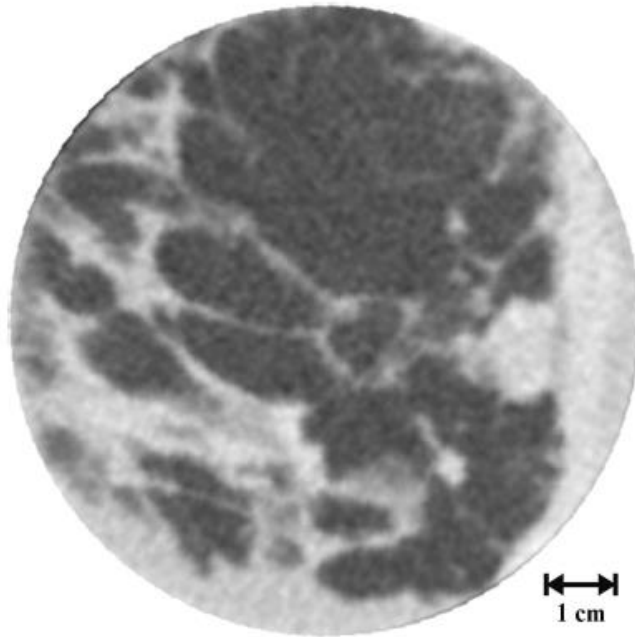


Ca in collagen

fat

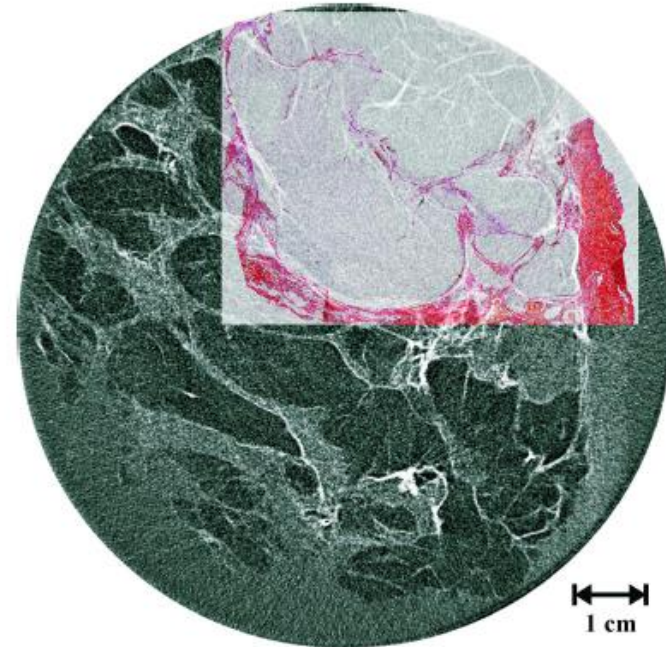
FIRST LOW DOSE CT DEMONSTRATION ON FULL MASTECTOMY

Conventional



MGD=6.9 mGy

Phase contrast (ABI)



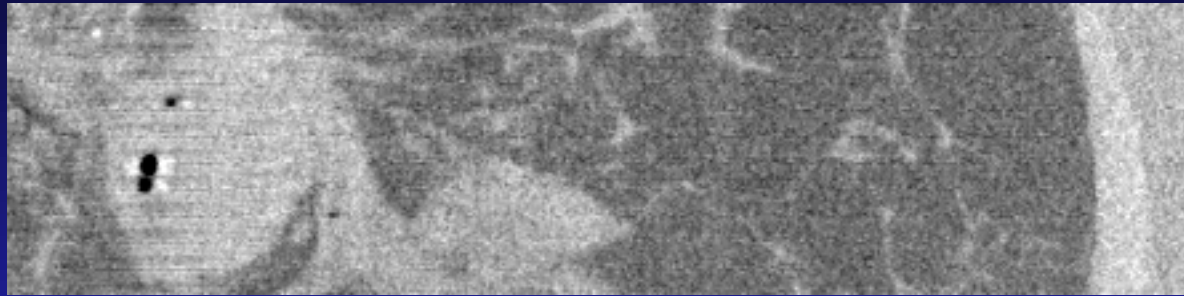
MGD=1.9 mGy

Full breast : 8 cm
33 keV

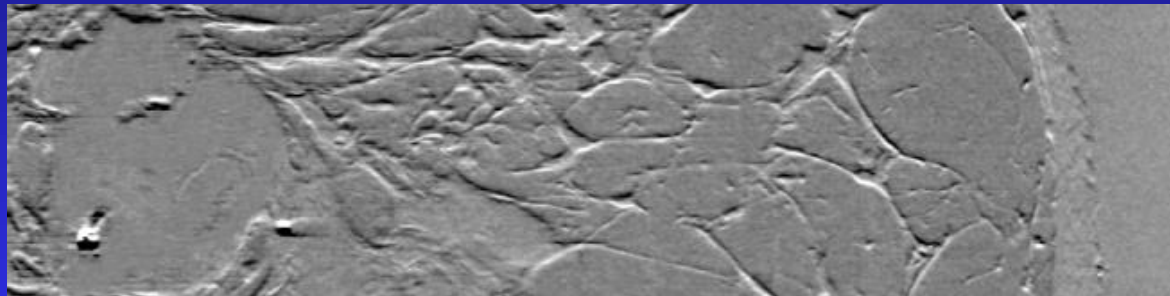
Keyriläinen et al. Radiology, 2008

Breast-CT: PCI-CT vs conventional CT vs histology

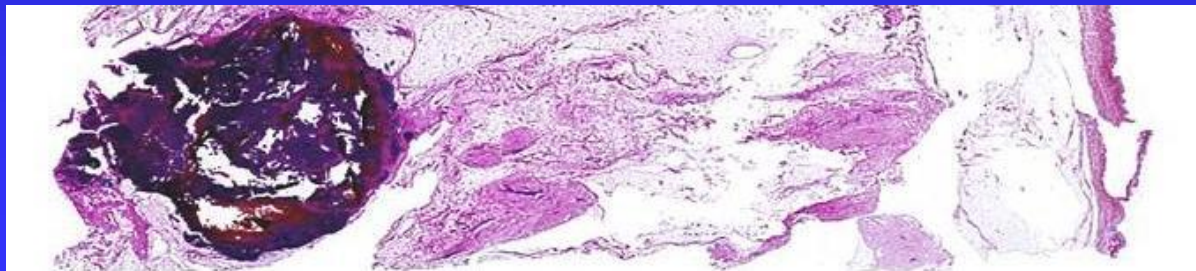
PCI CT outperforms conv. CT and it is in strong correlation with histology



Conventional Absorption



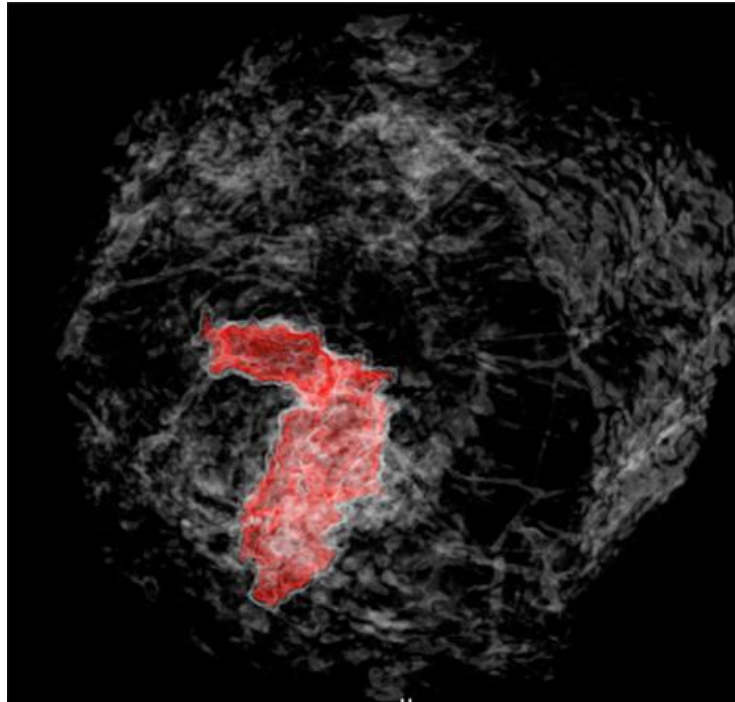
PCI CT



Histology

High-resolution, low-dose phase contrast X-ray tomography for 3D diagnosis of human breast cancers

Yunzhe Zhao^{a,1}, Emmanuel Brun^{b,c,1}, Paola Coan^{c,d}, Zhifeng Huang^a, Aniko Sztrókay^d, Paul Claude Diemoz^c, Susanne Liebhardt^d, Alberto Mittone^c, Sergei Gasilov^c, Jianwei Miao^{a,2}, and Alberto Bravin^{b,2}



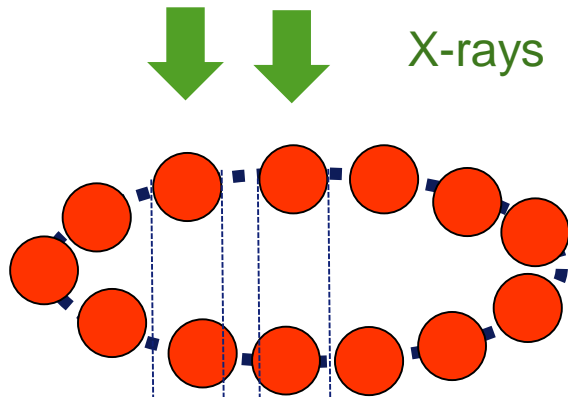
PNAS | November 6, 2012 | vol. 109 | no. 45 | 18293

Phase contrast CT
+ iterative reconstruction method

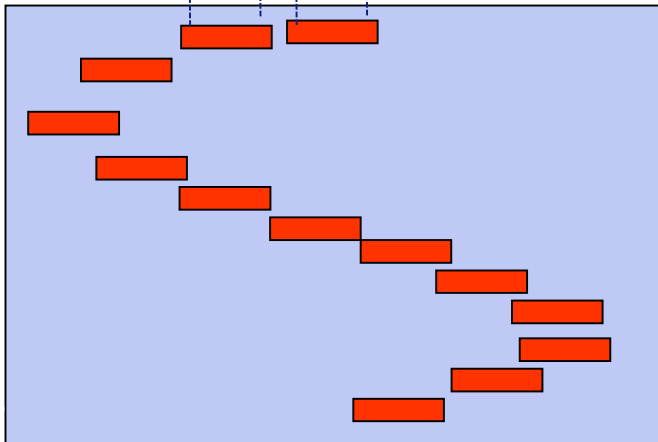
Dose = 2.0 ± 0.1 mGy
25 times dose saving vs clinical
breast CT at same resolution

CT BASIC PRINCIPLES

Rotating sample



Detector



3D image



Computing
(reconstruction
algorithms)



0°



Sinogram

360°

□ LOW DOSE CT

Combination of 3 ingredients:

“Phase contrast
imaging”

+

Advanced CT
reconstruction algorithms

+

High X-ray
energies



Highly sensitive
imaging techniques



Iterative algorithms for CT
reconstruction - less
projections than normally used



Tissues more
radio-transparent
-> less dose

- **Breast imaging needs high resolution**

- High number of projections for CT (Shannon Nyquist criterion):

$$\text{Proj} = \frac{D\pi}{p^2}$$

D: sample thickness
P: pixel size

- **Can we reduce the number of projections?**

2 possible strategies :

- To reduce the number of projections for a CT data set:
 - Shannon-Nyquist criterion not valid anymore
- To reduce the number of photons onto the detector per each angular projection

REDUCING THE NUMBER OF PROJECTIONS OF A CT DATA SET

32 projections



64 projections



128 projections



256 projections



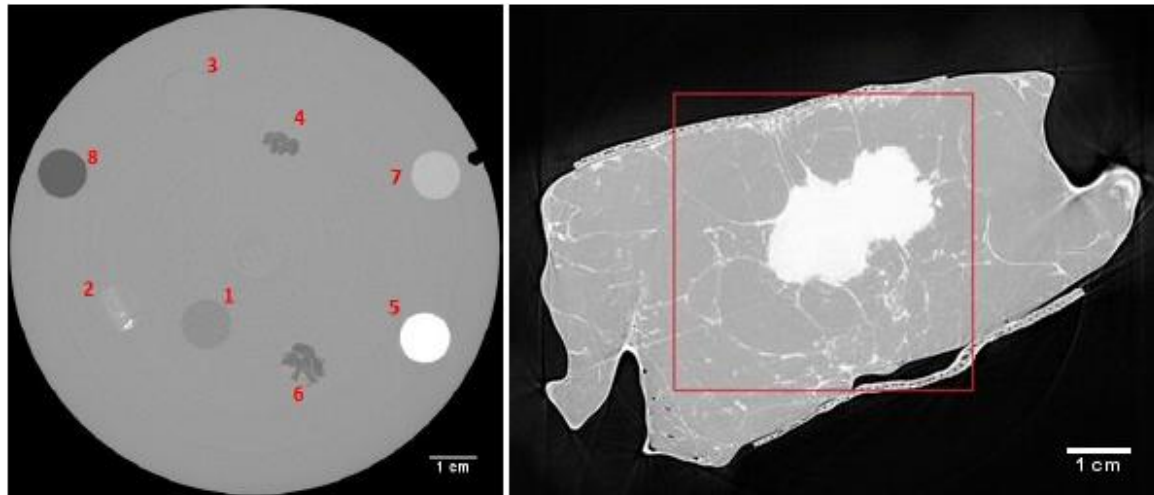
512 projections



1024 projections

Using FBP: prone to the appearance of artefacts

- **Filtered Back Projection (FBP)**
- Simultaneous Iterative Reconstruction Technique (SIRT)
- Simultaneous Algebraic Reconstruction Technique (SART)
- Conjugate Gradient Least Squares (CGLS)
- Total Variation (TV) minimization
- Iterative FBP algorithm based on the image histogram updates
- **Equally Sloped Tomography (EST)**



S. Pacile et al, *Biomed Opt Express*. 2015 Aug 1; 6(8): 3099–3112

REDUCING THE NUMBER OF PROJECTIONS

Table 4. Qualitative assessment of the considered images performed by expert supervisors.

	Radiol. 1	Radiol. 2	Radiol. 3	Pathologist	Mean Score
FBP	1	1	1	1	1
FBP-ITER	1	1	1	0.5	0.87
SIRT	1.5	1	1.5	1.75	1.43
SART	1.5	1.25	1.5	1.75	1.5
CGLS	1	1.25	1.5	1.5	1.31
EST	1	1.25	1.5	1.5	1.31
phr FBP-ITER	3	3	2.5	2	2.62
phr FBP-ITER <i>Epan17</i>	2.5	3.25	2.5	2.5	2.68
phr FBP-ITER <i>Susan5</i>	2.5	3.25	3	2.5	2.81
phr TV-MIN	1.5	2.75	2.75	2.75	2.43
phr FBP	2.5	2.5	2.75	3.5	2.81
phr SIRT	3.25	3.25	3.5	3	3.25
phr SART	3.25	3.25	3	3	3.12
phr CGLS	2.5	3.25	3	3	2.93
phr EST	3.5	3.25	3.5	3.5	3.43

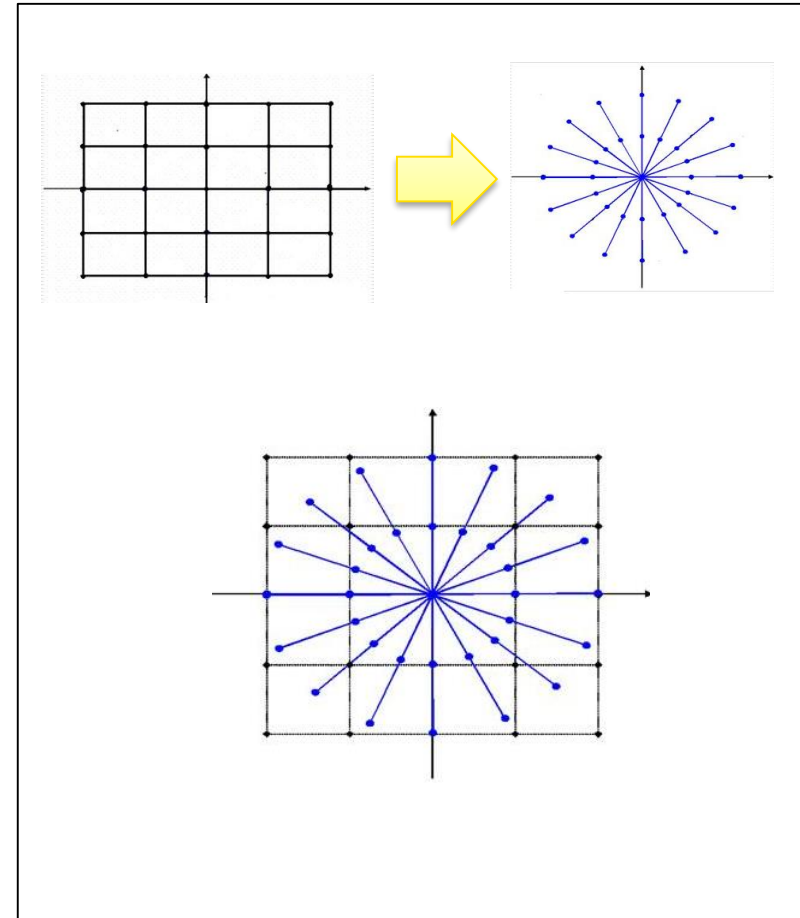


0: worst case; 4: best image

All algorithms available in X-TRACT software:
<http://www.ts-imaging.net/Services/SignUp.aspx>

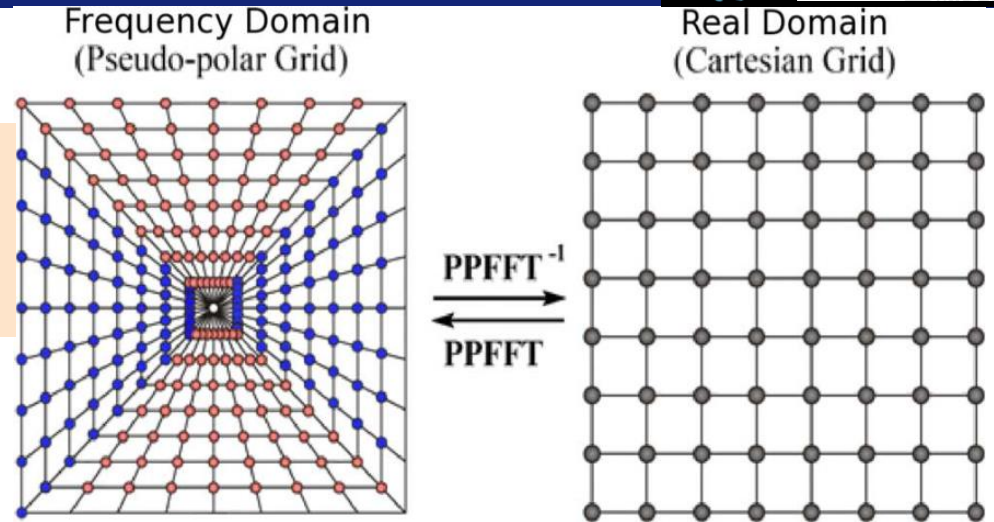
Observation:

- Real space image is in Cartesian grid while the Fourier space data is in Polar Grid
- There is no exact and direct FFT between polar and Cartesian Grid [1]



[1] Briggs, W.L., Henson V.E. The DFT: An owners' Manual for the Discrete Fourier Transform. SIAM, Philadelphia. 1995

Idea : “a polar like” grid that enables direct and exact Fourier transform
 => **PSEUDO POLAR GRID**



- Grid points in the Fourier domain are lying on the **equally-sloped lines instead of equally-angled lines**
- $N \times N$ Cartesian grid \rightarrow $2N \times 2N$ Pseudo polar grid (PPG) points
- There exist a PPFFT between PPG and Cartesian Grid
 - algebraically exact
 - geometrically faithful
 - Invertible

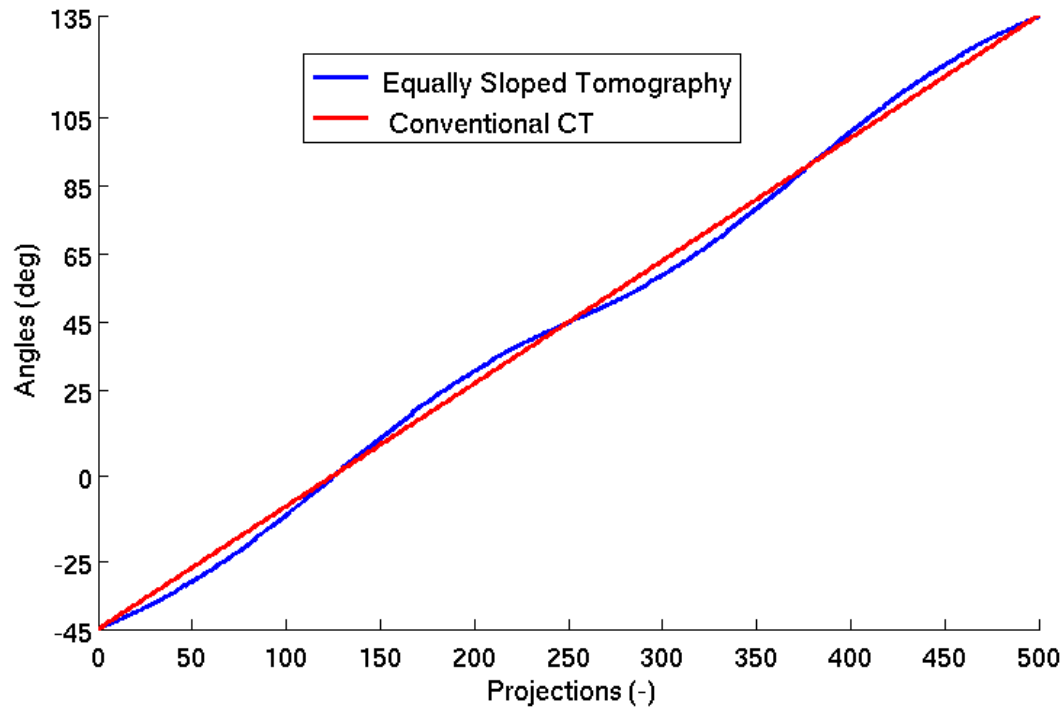
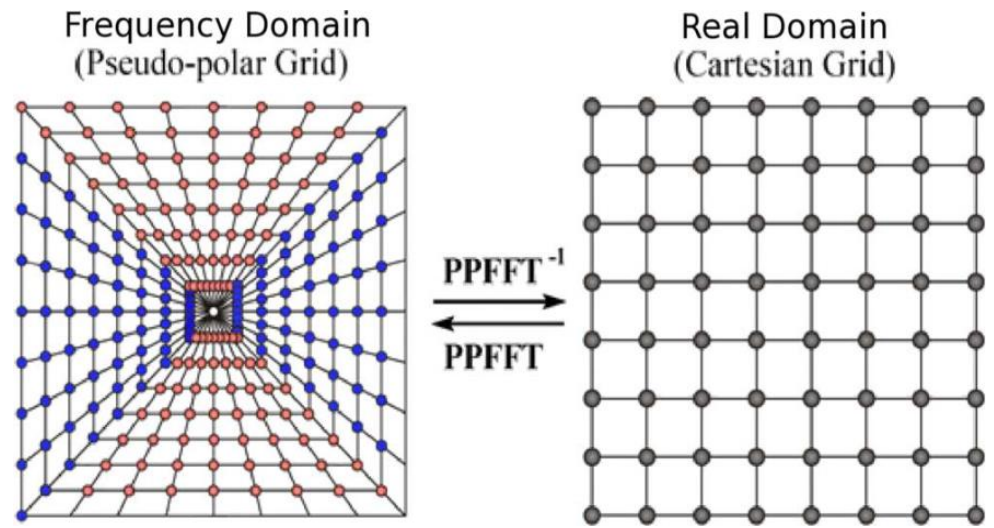
Slides provided by Prof. P. Coan

Miao et al. Phys Rev B ,72 (2005)

PNAS, Zhao, Brun, Coan et al., 109 (45) 6 Nov 2012



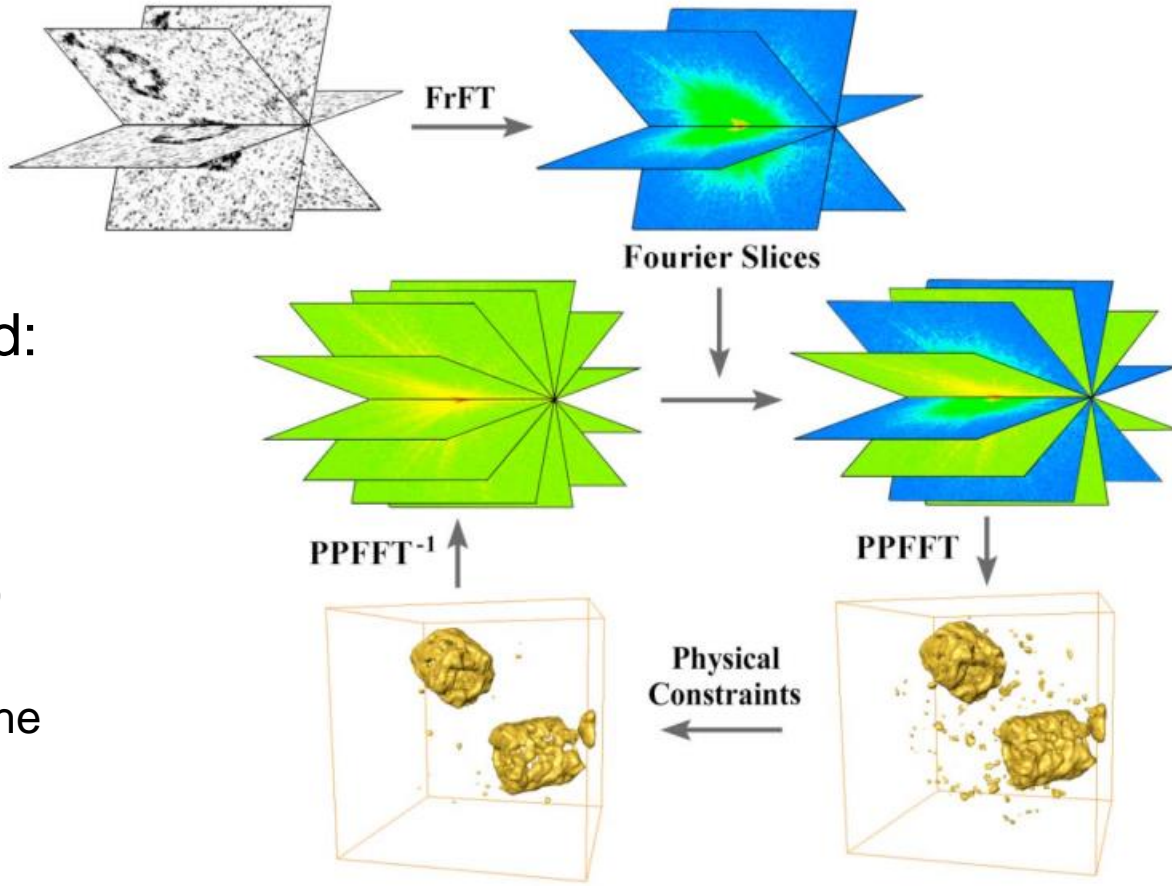
Idea : “a polar like” grid that enables direct and exact Fourier transform
=> **PSEUDO POLAR GRID**





EST iterative algorithm

Starts with the conversion of the projections to Fourier slices in the pseudo polar grid fractional FFT



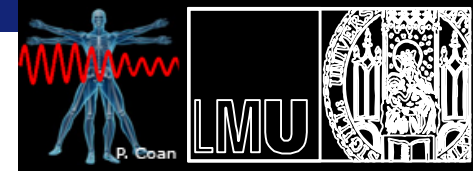
Iterative process is initiated:

- Inverse PPFFT is applied to the frequency data
- A new object is obtained through constraints. Forward PPFFT onto modified image
- Frequency data is updated with the measured Fourier slices

Real domain constraints:

- Minimization of the coefficients
- Real values as result

Iterations are monitored by an error function



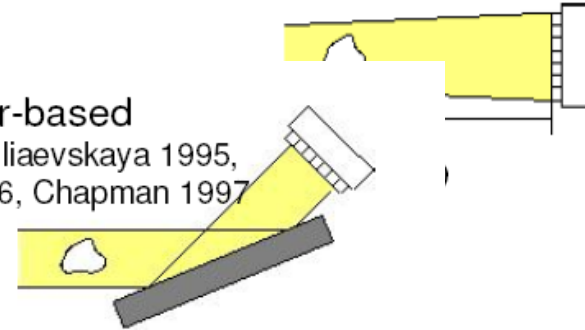
→ On both synthetic and experimental data

→ Different Phase Contrast Imaging techniques **Propagation-based**

Snigirev 1995, Wilkins 1995, Cloetens 1996

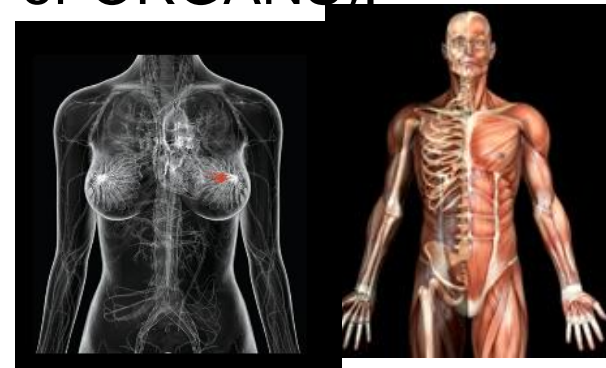
- Propagation based imaging
- Analyzer based imaging

Analyzer-based
Ingal & Beliaevskaya 1995,
Davis 1996, Chapman 1997



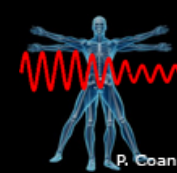
→ Different clinical cases (FULL JOINTS or ORGANS):

- Breast imaging
- Musculoskeletal imaging

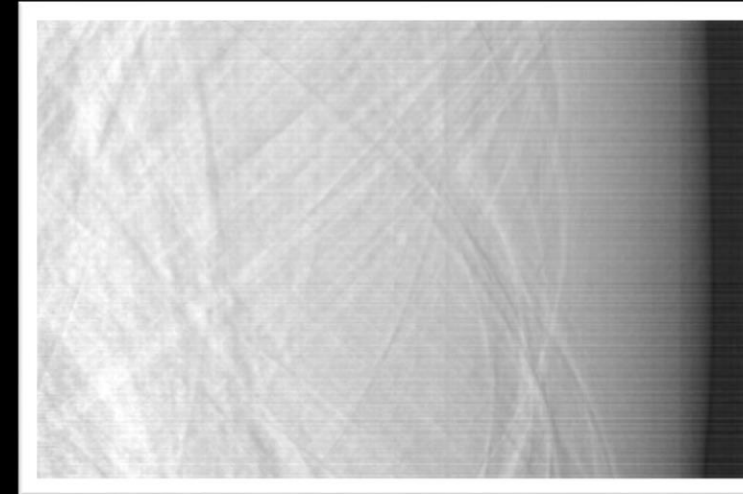
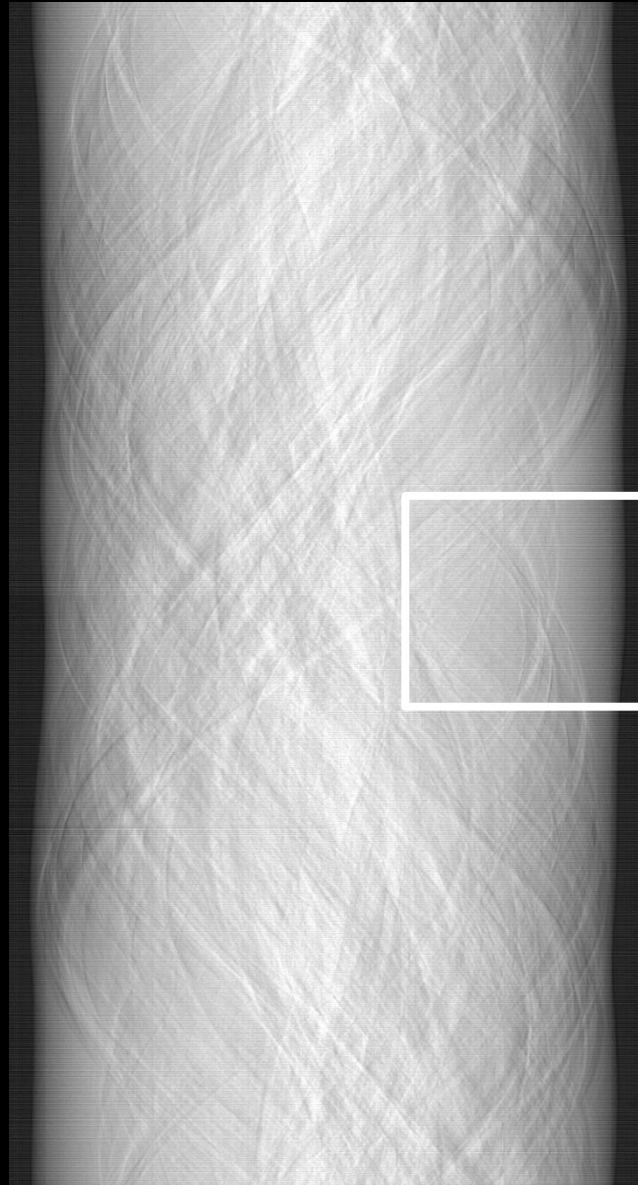


Slides provided by Prof. P. Coan

The raw data



The sinogram

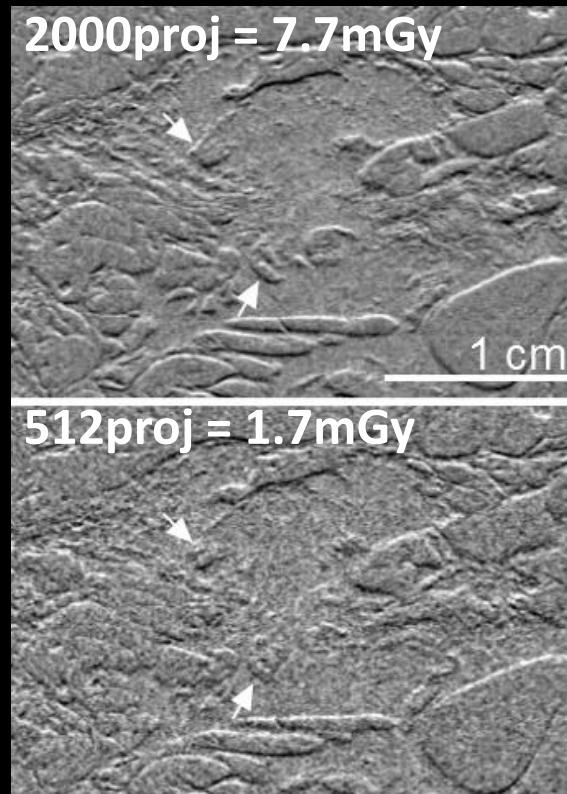


Visual Comparison

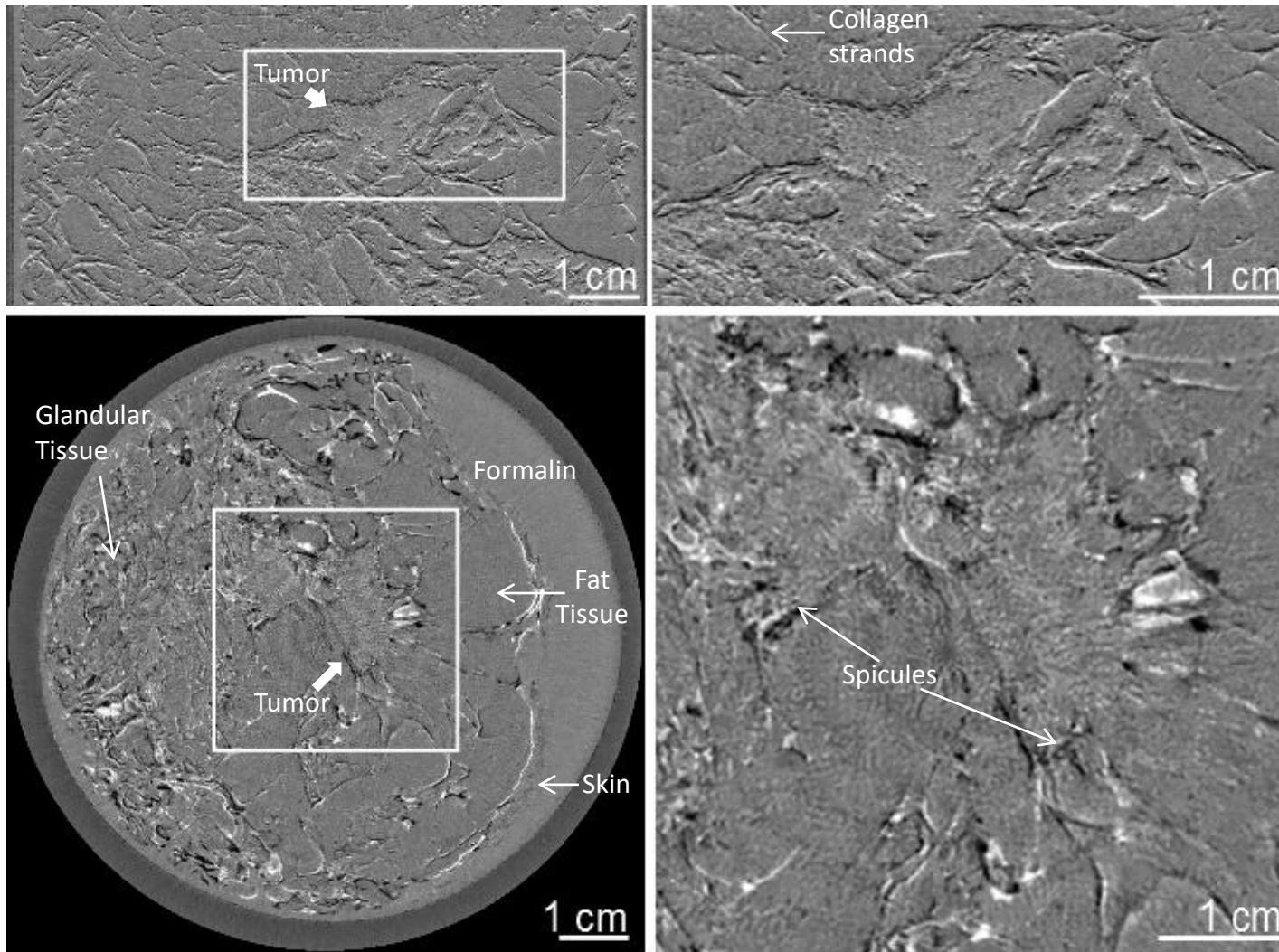
Zoomed view in a 92 μm thick slice an excised full human tumor bearing breast

FBP

- FBP - 512 exhibits high noise degraded features and blurred boundary of the tumour



Result of reconstruction by EST 512projections



MGD
1.7mGy

Quantitative Comparison



Blind Test made by 5 radiologists (Radiology department of Ludwig Maximilians University)

Radiologist were asked to mark form 1 (worst) to 5 (best) on the following criteria

	FBP 512	EST 200	FBP2000	EST512
Image quality	2.2 ± 0.4	2.7 ± 0.9	4.3 ± 0.9	4.5 ± 0.5
Sharpness	3.3 ± .0	2.2 ± 0.8	4.0 ± 0.7	4.3 ± 0.5
Contrast	3.0 ± 0.7	3.4 ± 0.9	4.0 ± 0.5	4.8 ± 0.4
Evaluation of different structure	2.7 ± 0.5	2.9 ± 1.	4.1 ± 0.6	4.8 ± 0.4
Noise	1.8 ± 0.7	3.3 ± 0.8	4.2 ± 0.7	4.8 ± 0.3

3D CT breast tumor detection at high resolution and at a dose even lower than conventional 2D mammography (~3.5 mGy)!

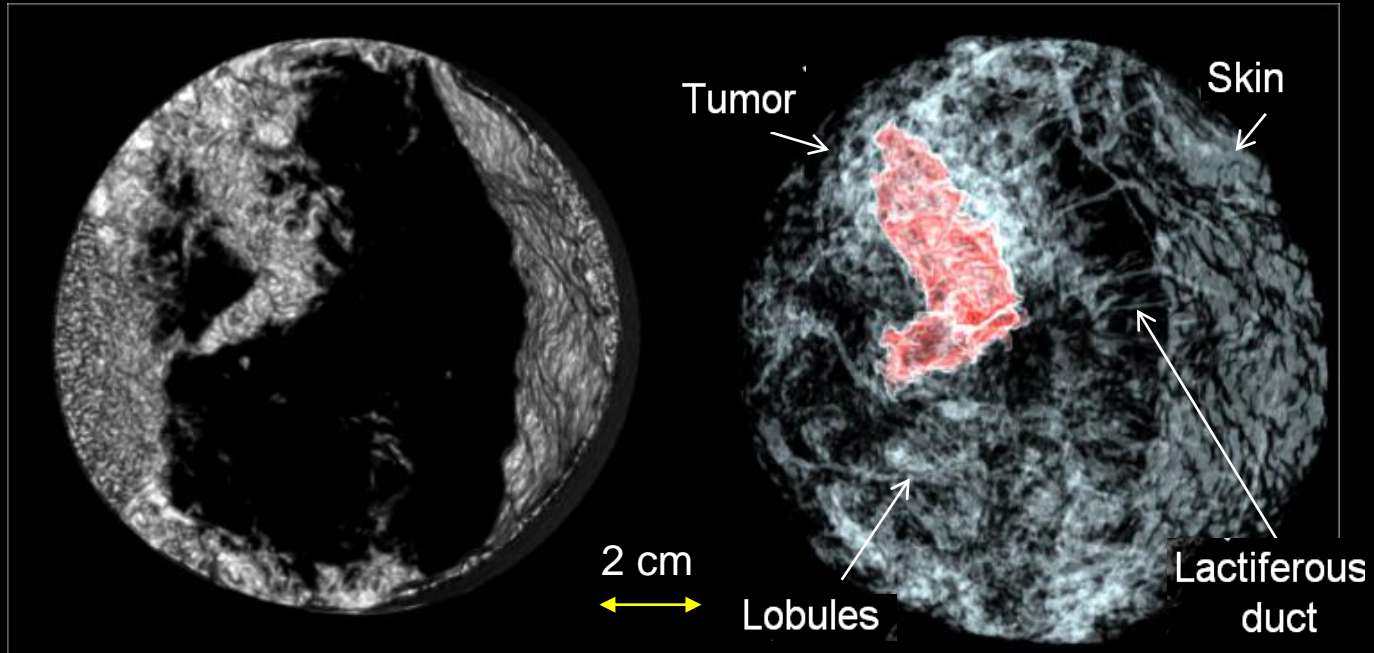
Fourier based iterative Equally Slopped Tomography (EST) algorithm

Conventional CT
Dose 49 ± 1 mGy

Phase contrast CT + EST
Dose = 2.0 ± 0.1 mGy



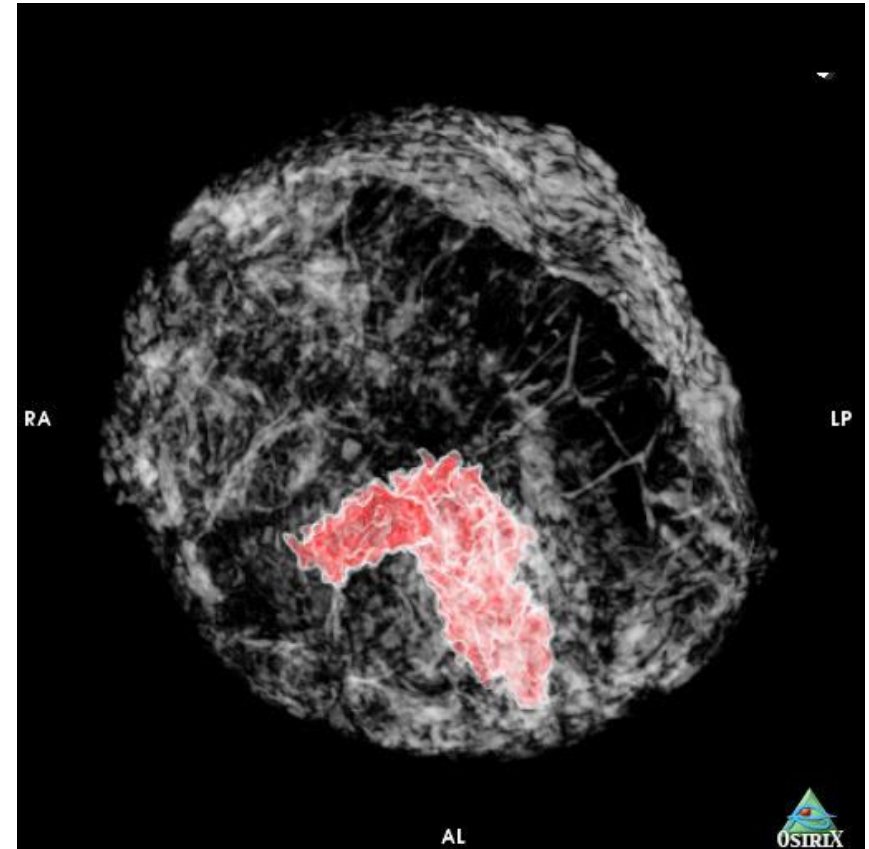
UCLA



25 times dose saving vs clinical breast CT at same resolution

Summary

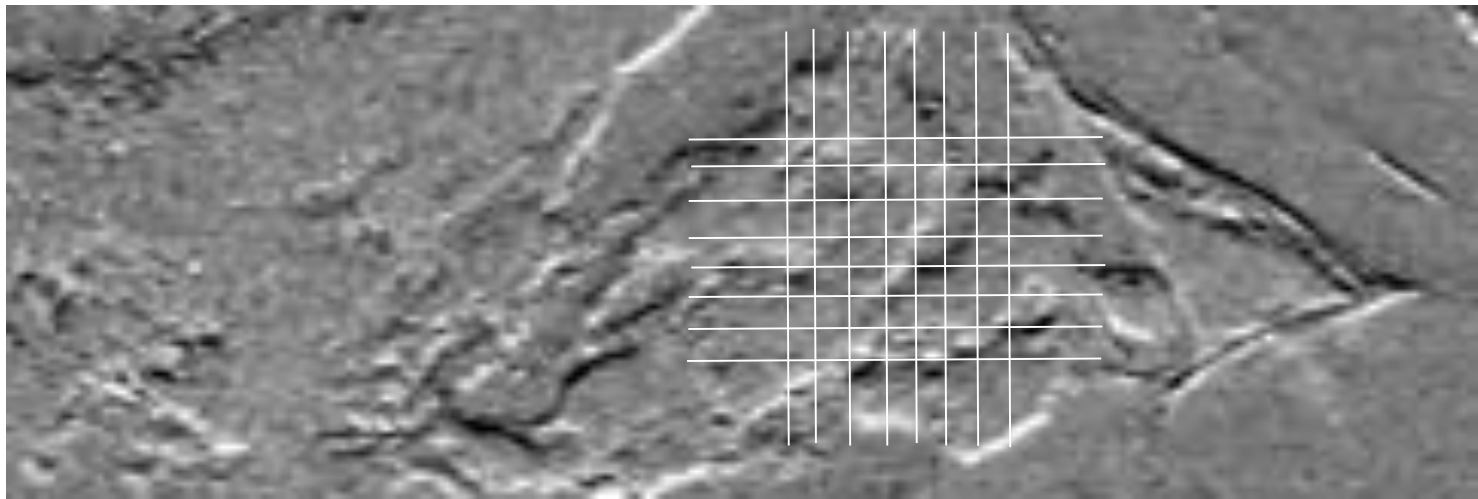
- 3D information of soft tissues at **higher resolution** and **better contrast**, but also deliver **less radiation** doses to the sample
- A step towards the clinical application of PCT for 3D screening and diagnosis of human breast cancer
- Very low dose (**<1mGy**) 3D imaging is possible if one is ready to loose a bit of spatial resolution and noise



PNAS, Zhao, Brun, Coan et al., 109 (45) 6 Nov 2012

Sparsity

image is intrinsically sparse when it can be approximated as a linear combination of a small number n of basis functions, with $n \ll N$, where N is the image dimensionality



Good case: when image has large constant parts: the basis can be small pieces varying only on the borders

How many patches?

$m \times m \ll N \times N$ (pixel size)

- Fast calculation
- Image not well reproduced
- Very low noise (noise has little sparsity)

$m \times m \gg N \times N$ (pixel size)

- Heavy computation
- Image well reproduced
- Very smooth transition at the patches borders if the patches are overlapping
- Also noise is reproduced, to be treated with a denoisy method

Submethods:

- **Dictionary learning**
- **Total Variation penalization (TV)**: introduces a regularization parameter

All mathematics can be found in

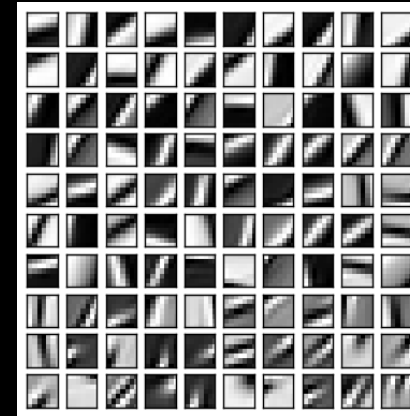
A. Mirone, E. Brun, P. Coan. PlosOne, 9(12) e114325

Dictionary Learning reconstruction



Idea of the method :

- To create a database of patchworks starting from images close to the images to be reconstructed
- To decompose the slice to be reconstructed in a patchwork of sub-images
- To express a given sub-image at position “ r ” as a linear combination of the basis patches
- To find the solution which gives the maximum Likelihood by minimizing the number of entries in the dictionary
- Minimization is done toggling between slice and sinogram
- A regularization included to assure fidelity



Dictionary “learnt” from Lena image and used for reconstructing the image of interest

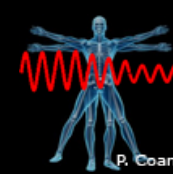


Noisy image



Denoised image

Reconstructing Lena



- **Experiment :**
 - 512*512 pixel Lena image
 - 80 projections
- **Remark :**
 - To avoid aliasing 800 projections should be used (Nyquist-Shanon sampling criterion)



Lena image to reconstruct

Results



FBP



EST



TV

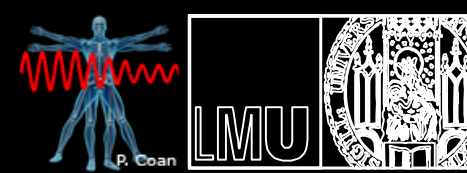


DL

NO noise

80 projections

Zoom views in two different image regions



FBP

EST

TV

DL

Original

Results



FBP



EST



TV



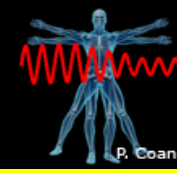
DL

Noisy data

Additive White Gaussian
Noise = 0.3% max of
sinogram

80 projections

Zoom views in two different image regions



Additive White Gaussian Noise = 0.3% max of sinogram



FBP

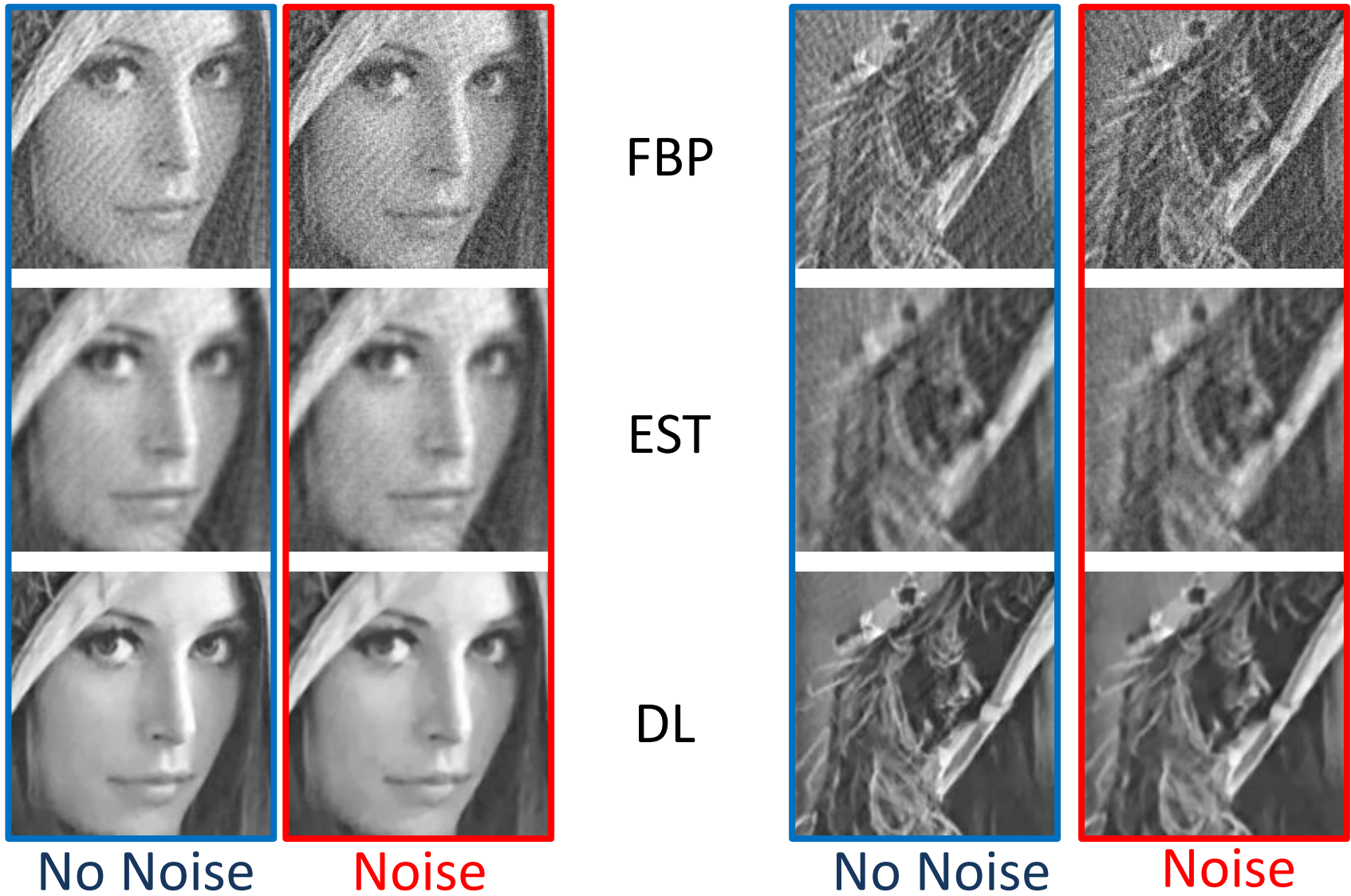
EST

TV

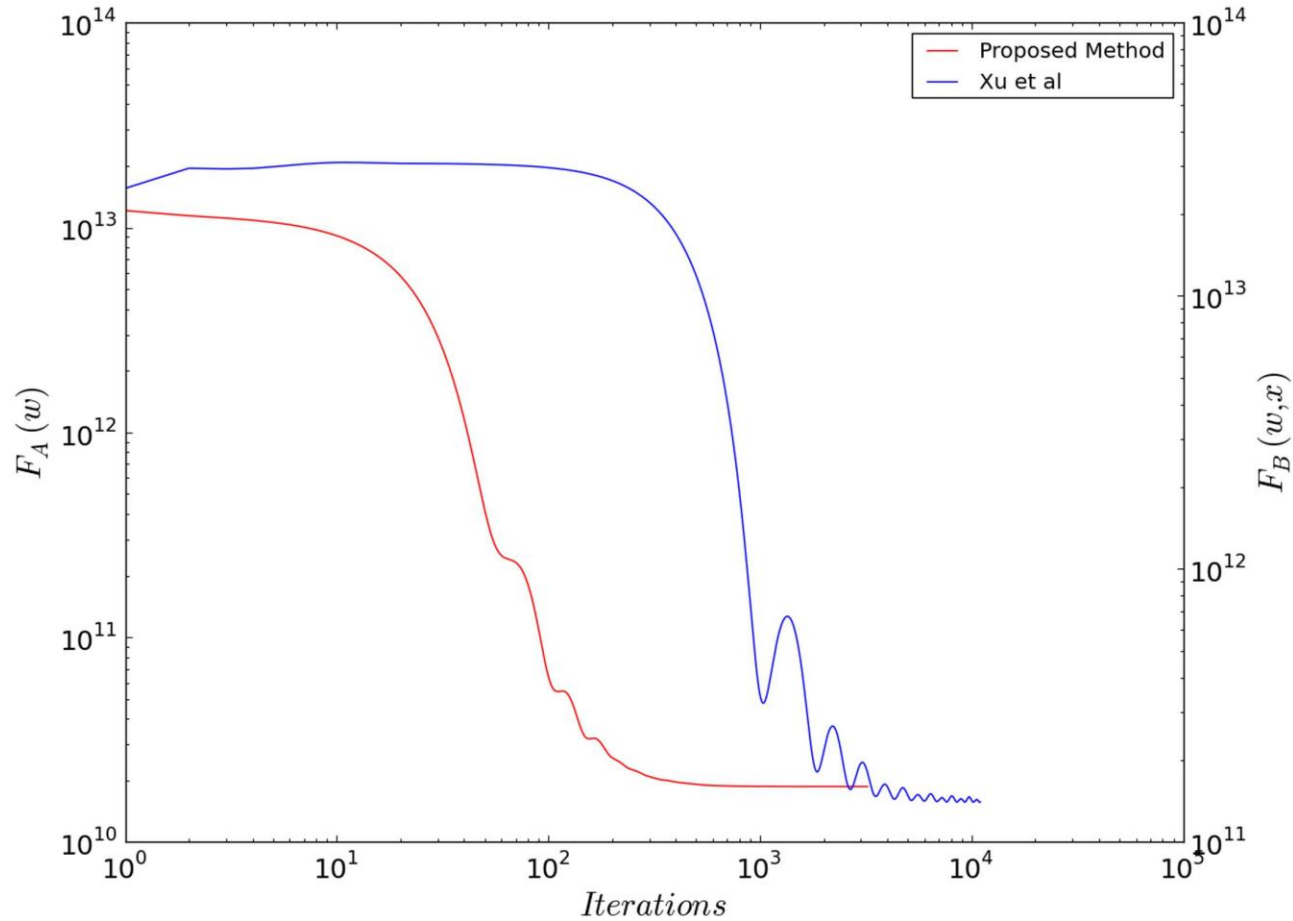
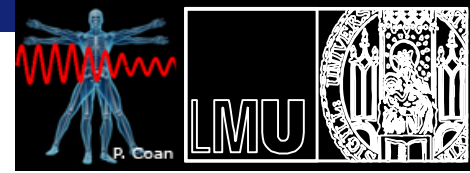
DL

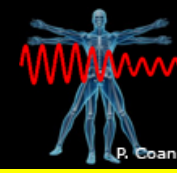
Original

Direct comparison

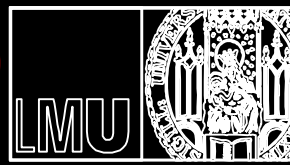


THE IMPORTANCE OF THE FAST CONVERGING



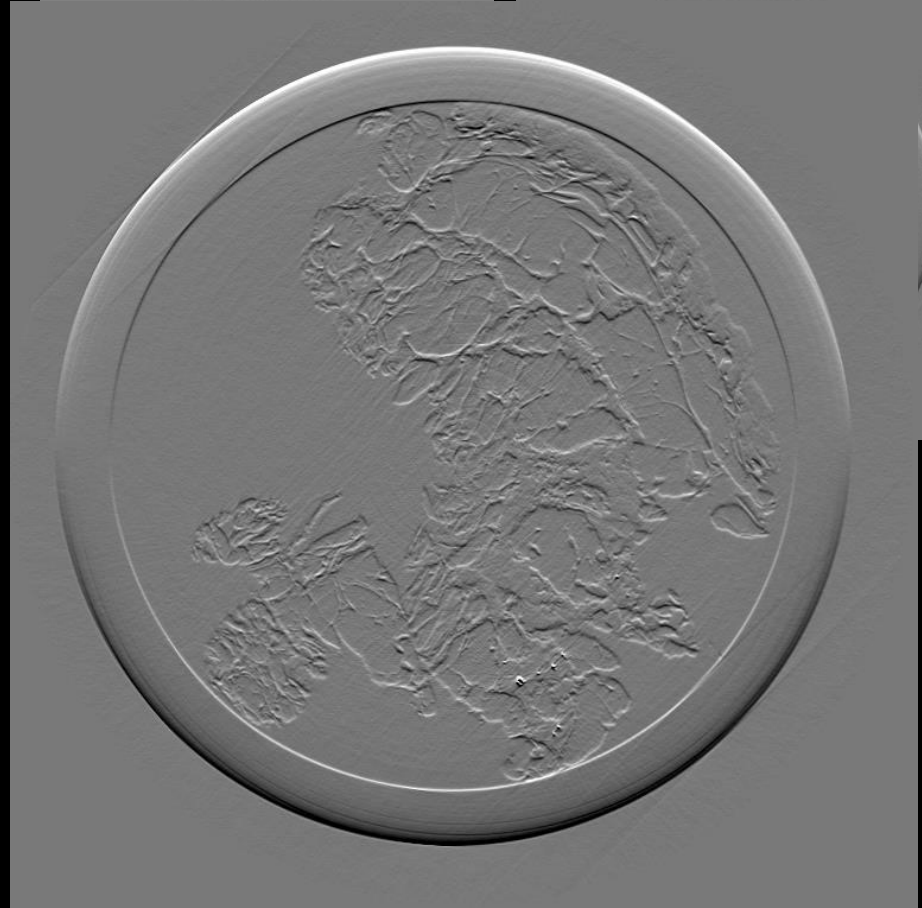
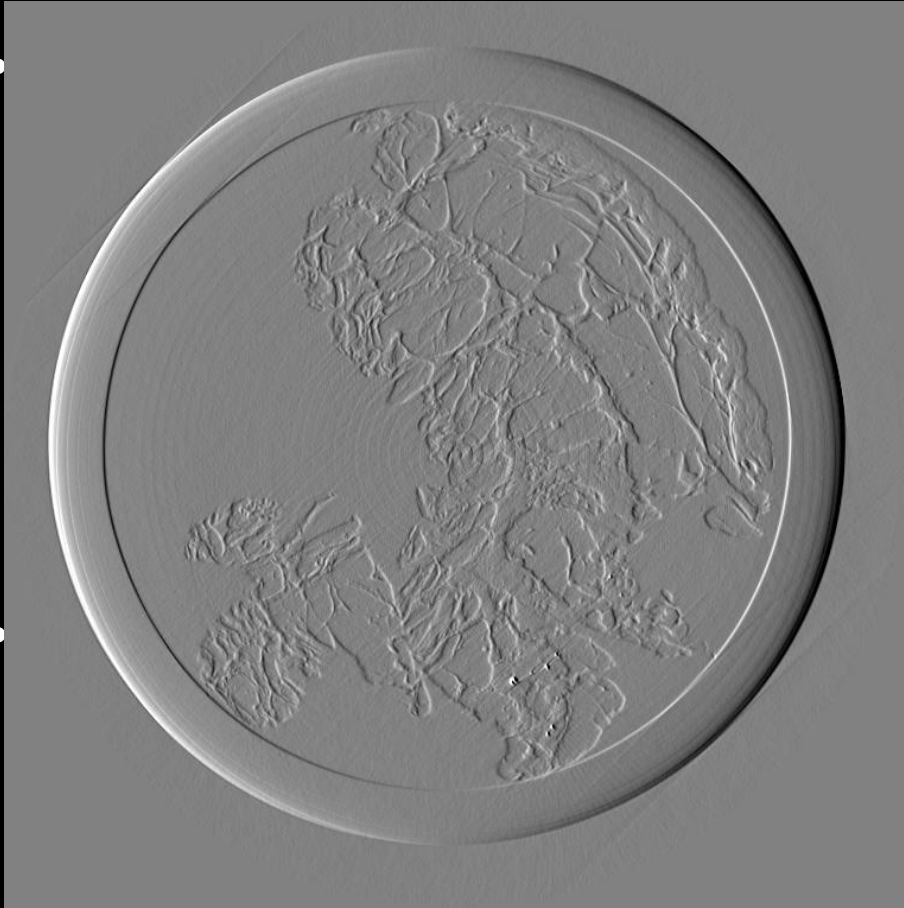
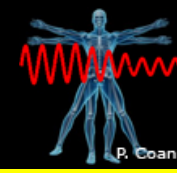


P. Coan



APPLICATION ON EXPERIMENTAL DATA

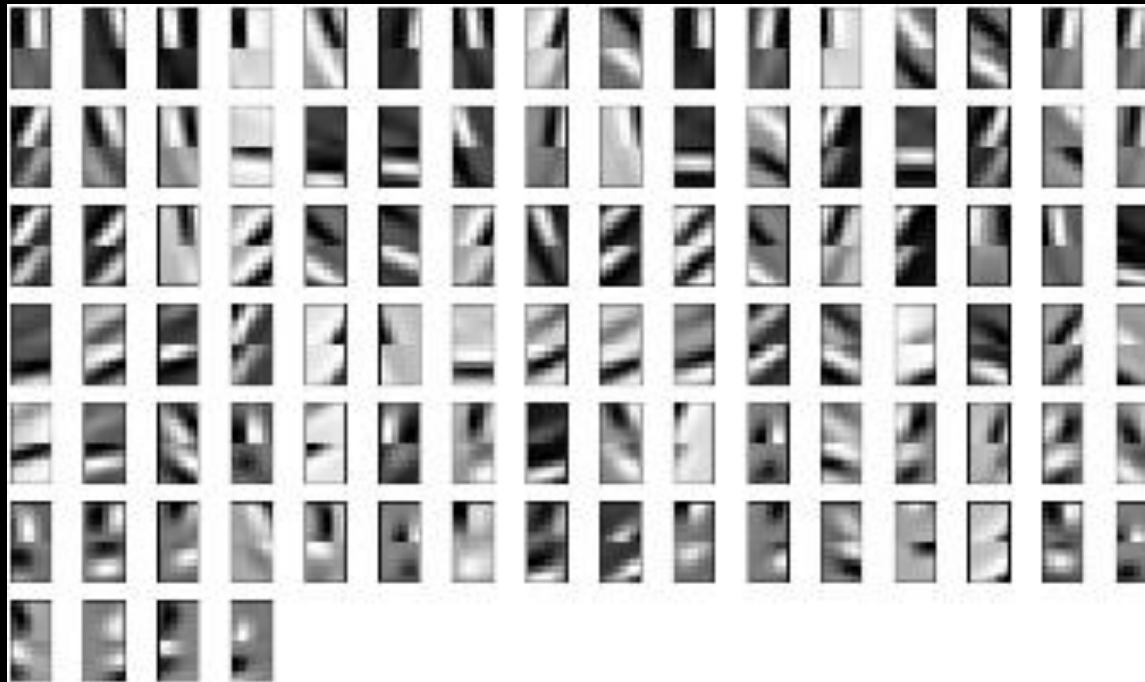
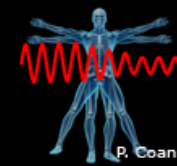
Reconstructing phase gradient images



Shannon criterion: 2335 projections
(pixel: 47 microns)

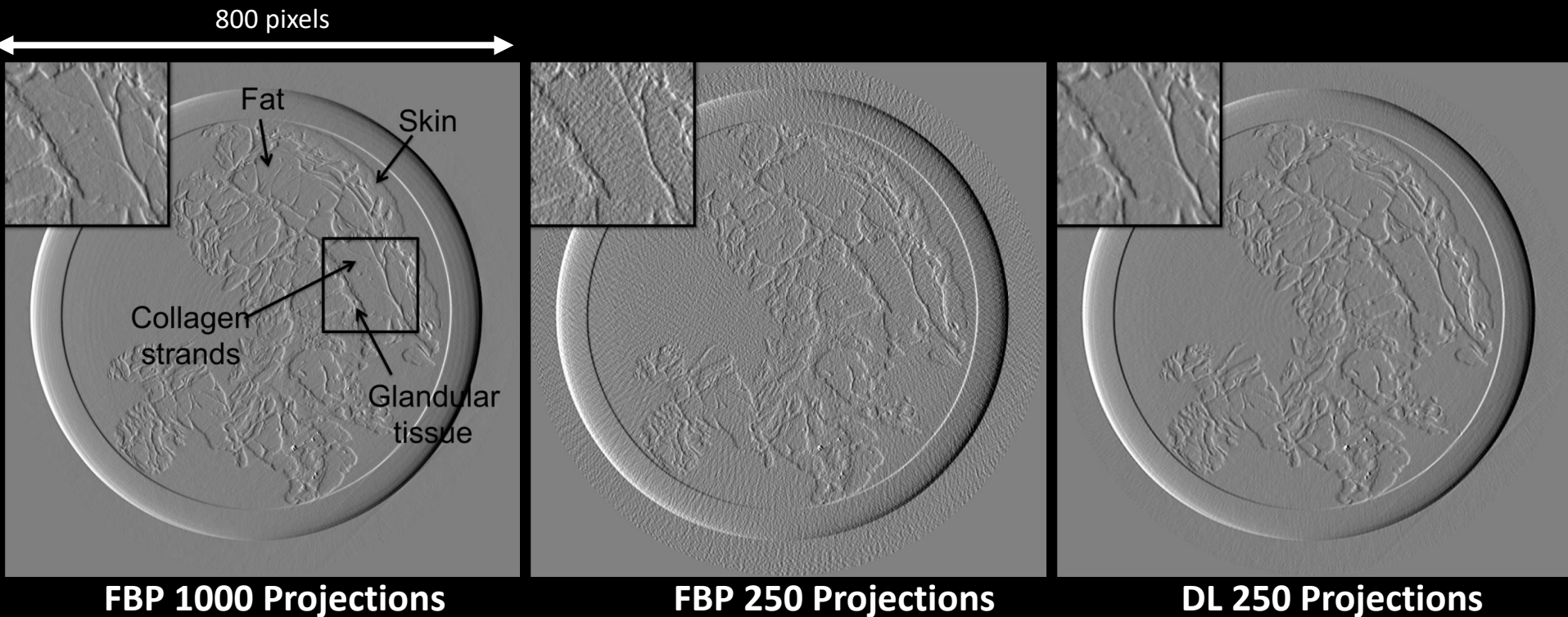
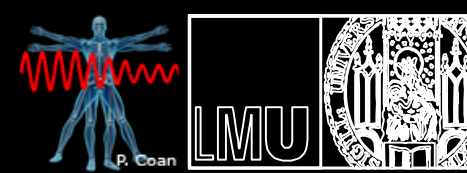
Diameter: 7 cm

Vectorial Set of Patches



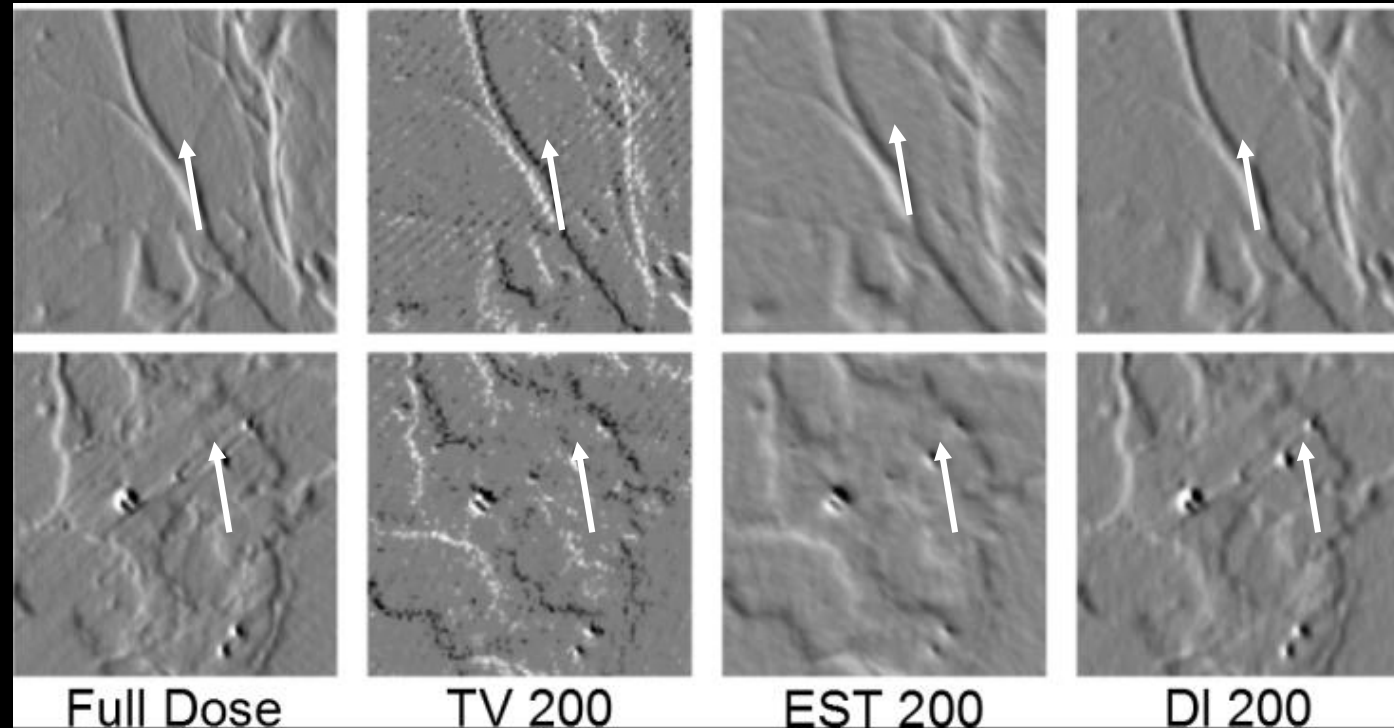
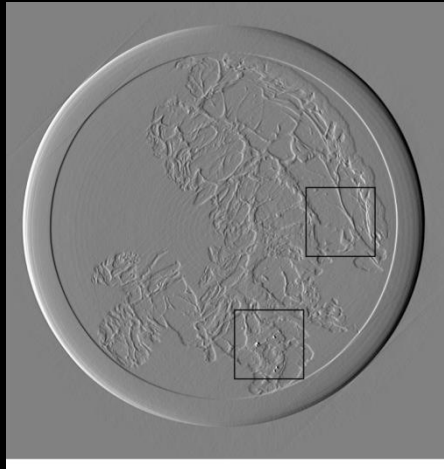
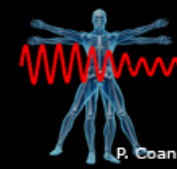
Set of $2 * 7 * 7$ pixels patches learnt from another breast sample

Phase Contrast Reconstruction using DL



Analyzer Based Imaging of a full (7cm) human tumor bearing breast tumor

Closer Look



Small Structures are preserved in the Dictionary Learning reconstructions
Global Image quality is higher in DL

Tomographic reconstruction of the refractive index with hard X-rays: an efficient method based on the gradient vector-field approach

Sergei Gasilov,^{1,*} Alberto Mittone,^{1,2} Emmanuel Brun,^{1,3} Alberto Bravin,³, Susanne Grandl,² Alessandro Mirone,³, and Paola Coan^{1,2}

Optics Express Vol. 22, Issue 5, pp. 5216-5227 (2014)

Phase retrieval converting the problem to Poisson equation, robust to noisy data

Boundary value problem for phase retrieval from unidirectional X-ray differential phase images

Sergei Gasilov,^{1,*} Alberto Mittone,^{2,3,4} Annie Horng,⁴ Alberto Bravin,³ Tilo Baumbach,¹ Tobias Geith,⁴ Maximilian Reiser,⁴ and Paola Coan^{2,4}

18 May 2015 | Vol. 23, No. 10 | DOI:10.1364/OE.23.013294 | OPTICS EXPRESS 13294

Application of a finite element technique to solve The boundary value problem in phase retrieval

On the possibility of quantitative refractive-index tomography of large biomedical samples with hard X-rays

Sergei Gasilov,^{1,*} Alberto Mittone,^{1,3} Emmanuel Brun,^{1,2} Alberto Bravin,² Susanne Grandl,³ and Paola Coan^{1,3}

1 September 2013 | Vol. 4, No. 9 | DOI:10.1364/BOE.4.001512 | BIOMEDICAL OPTICS EXPRESS 1512

PhC vs conventional CT: accuracy in refraction Index calculation in noisy data

A single-image method for x-ray refractive index CT

A Mittone^{1,2,4}, S Gasilov^{1,3}, E Brun^{1,4}, A Bravin⁴ and P Coan^{1,2}

Phys. Med. Biol. 60 (2015) 3433–3440

Fast and low dose phase retrieval using a single Image dataset

The problem of the radiation delivered

How to perform fast dose simulations?

Conventional Monte Carlo
Long computational time

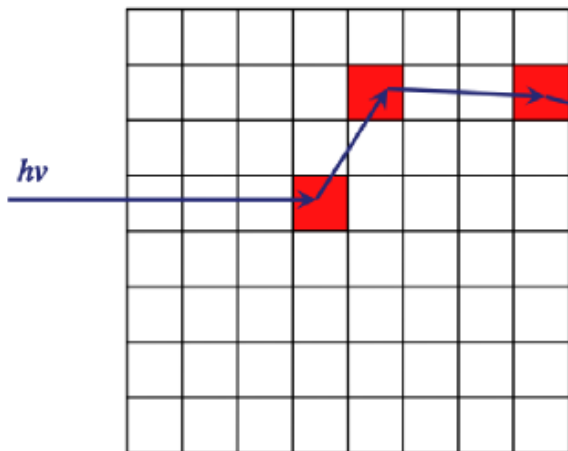


- The track-length estimator (TLE)
- Electrons production cut

How to perform fast dose simulations?

Conventional Monte Carlo
Long computational time

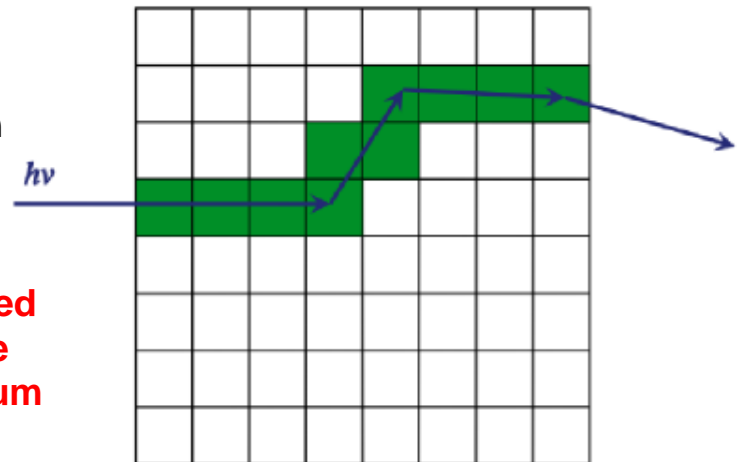
- The track-length estimator (TLE)
- Electron energy is deposited locally and are not tracked



Local deposition
vs
continuous deposition

$$D = \Phi E \frac{\mu_{en}}{\rho}$$

In charged
particle
equilibrium



- It requires fewer particles to converge
- Works when electron range is < spatial resolution (<100 keV)
- No significant energy escape (radiative, atomic deexcitation): $Z < 20$; $E < 1$ MeV

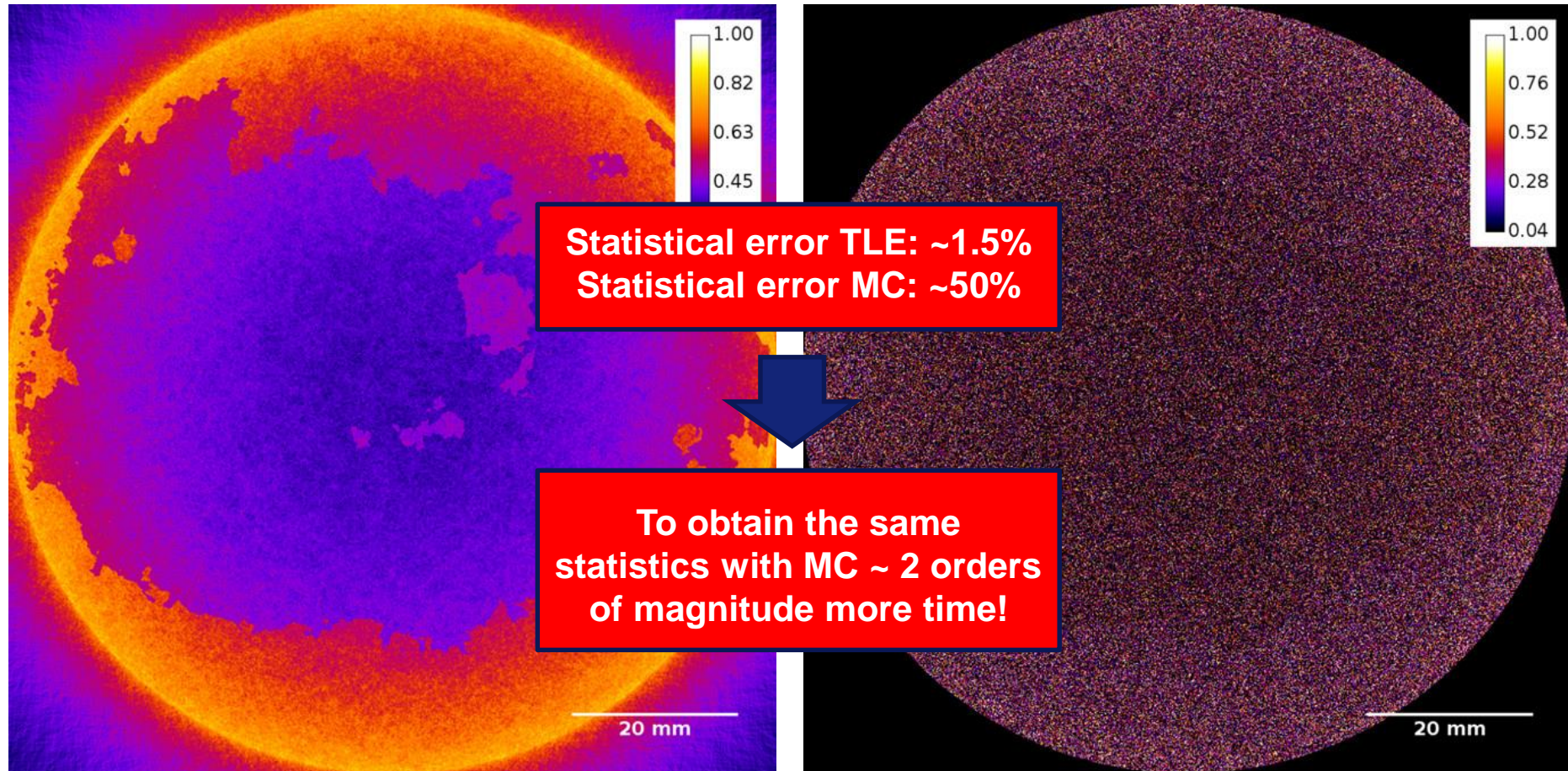
The TLE code (C++) has been
integrated in GATE (Geant4)

COMPARISON WITH STANDARD MONTE CARLO METHOD

10^7 events on segmented CT data of experimental breast sample

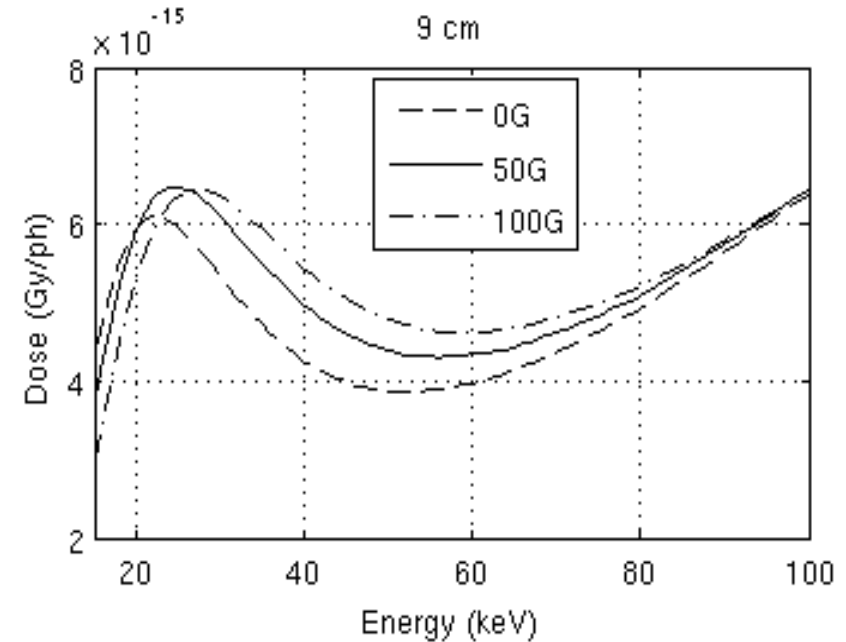
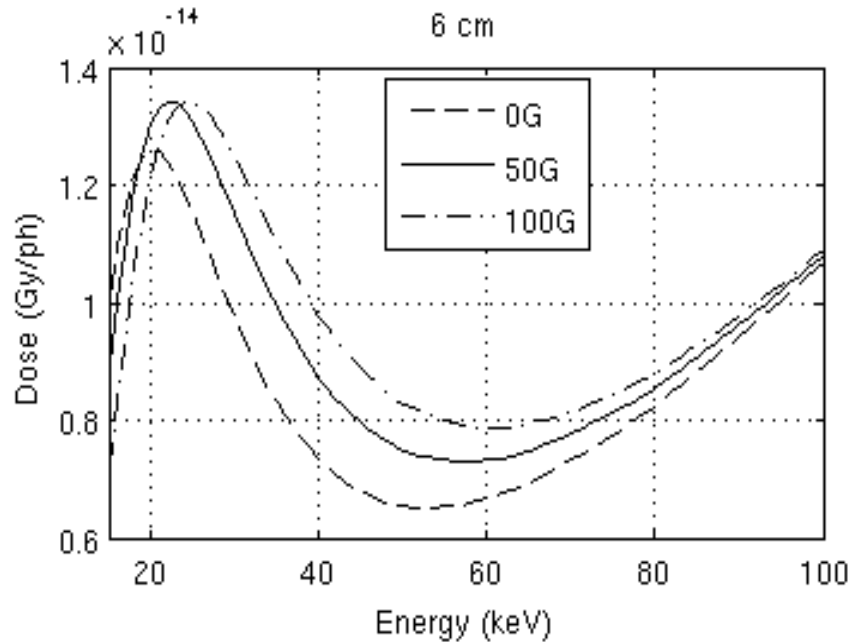
TLE Method^{8,9}

Standard Monte Carlo



⁸A. Mittone et al, *J. Synchrotron Radiat.* 2013.

⁹F. Baldacci, A. Mittone et al, *Z. Med. Phys.*, 2015.



Estimation of the average dose in a breast (monochromatic radiation):

- Range of energy: 15-100 keV
- Different geometries (thickness)
- Different compositions (fraction of glandular tissue)

A. Mittone et al, Phys. Med. Biol. **59** (2014) 2199–2217.

- S Fiedler, A Bravin, *Physics in Medicine and Biology* 49 175-188 (2004)
- M. Fernández, J. Keyriläinen, *Spectroscopy* 18 (2004) 167–176
- J. Keyriläinen, M. Fernández, *European Journal of Radiology*, 53, 226-237 (2005)
- M. Fernandez, J. Keyrilainen, *Phys. Med. Biol.* 50 (2005) 2991–3006
- A. Bravin, J. Keyriläinen, *Phys. Med. Biol.* 52 (8) 2197–2211 (2007)
- J Keyriläinen, M Fernández, *Radiology*, 2008: 249 (1) 321-327
- Fernández M, Suhonen H, *Eur J Radiol.* 68S (2008) S89-S94
- Keyriläinen J., Fernández M., *Journal of Synchrotron Radiation* 18, 689-696 (2011)
- Sztrókay A, Diemoz PC, *Phys Med Biol.* 2012 May 21;57(10):2931-42. Epub 2012 Apr 20.
- Y. Zhao, E. Brun, *PNAS* 2012, November 6, vol. 109, no. 45, 18290–18294
- P Coan, A Bravin *J. Phys. D: Appl. Phys.* 46 (2013) 494007
- A Mittone, A Bravin *Phys. Med. Biol.* 59 (2014) 2199–2217
- E. Brun, S. Grandl, *Medical Physics* 41, 111902 (2014)
- K. Bliznakova, P. Russo, *Computers in Biology and Medicine*, 61 (2015) 62-74
- S Grandl, A Sztrókay-Gaul, *PLOS ONE* 2016 Jun 30;11(6):e0158306.
- Bliznakova K., Kamarianakis Z., *IFMBE Proceedings*, 57, 367-371 (2016)
- Bliznakova K., Mettievier G., *Lecture Notes in Computer Science* 9699, 611-617(2016)
- Bliznakova K., Russo P., *Physics in Medicine and Biology* 61, 6243-6263(2016)
- J. Keyrilainen, A. Bravin, *Acta Radiologica* 2010 51 (8) 866-884
- Gasilov S, Mittone A, *Opt Express.* 2014 Mar 10;22(5):5216-27. doi: 10.1364/OE.22.005216.
- A. Mirone, E. Brun *PLOS ONE* 2014 vol.9, art 0114325. DOI:10.1371/journal.pone.0114325
- Baldacci F, Mittone A, *Z Med Phys.* 2015 Mar;25(1):36-47
- A. Mittone, S. Gasilov, *Physics in Medicine and Biology* 60 (2015) 3433–3440
- Gasilov S, Mittone A, *Opt Express.* 2015 May 18;23(10):13294-308.
- S. Gasilov, A. Mittone, *Biomedical Optics Express* 2013 Vol. 4, No. 9 1512-1518
- A. Mittone, F. Baldacci, *J. Synchrotron Rad.* (2013) 20, 785–792
- A. Olivo, P. C. Diemoz, and A. Bravin *Optic Letters* (2012) Vol. 37, No. 5
- P. C. Diemoz, M. Endrizzi, *Physical Review Letters* 110, 138105 (2013)